Mineralogy, geochemistry and 40Ar-39Ar geochronology of the Barda and Alech complexes, Saurashtra, northwestern Deccan Traps: Early silicic magmas derived by flood basalt fractionation

Journal:	*Geological Magazine*
Manuscript ID	Draft
Manuscript Type:	Original Article
Date Submitted by the Author:	n/a
Complete List of Authors:	Cucciniello, Ciro; Università di Napoli, Scienze della Terra, dell'Ambiente e delle Risorse Choudhary, Ashwini; Institute Instrumentation Center, Indian Institute of Technology Roorkee Pande, Kanchan; Department of Earth Sciences, Indian Institute of Technology Bombay, Powai, Mumbai Sheth, H.C. ; Indian Institute of Technology, Dept. of Earth Sciences
Keywords:	Deccan Traps, Saurashtra, granophyre, rhyolite, Ar-Ar dating, petrogenesis

Mineralogy, geochemistry and ^{40}Ar-^{39}Ar geochronology of the Barda and Alech complexes, Saurashtra, northwestern Deccan Traps: Early silicic magmas derived by flood basalt fractionation

Ciro Cucciniello*[†], Ashwini Kumar Choudhary[§], Kanchan Pande[‡], Hetu Sheth[‡]

*Dipartimento di Scienze della Terra, dell'Ambiente e delle Risorse (DiSTAR), Università di Napoli Federico II, Complesso Universitario Monte Sant'Angelo, Via Cintia 26 (edificio L), 80126 Napoli, Italy

§Institute Instrumentation Center, Indian Institute of Technology Roorkee, Roorkee 247667 India

‡Department of Earth Sciences, Indian Institute of Technology Bombay, Powai, Mumbai 400076 India

Abstract

All continental flood basalt (CFB) provinces contain silicic (granitic and rhyolitic) rocks, which are of significant petrogenetic interest. These rocks can form by advanced fractional crystallization of basaltic magmas, crustal assimilation with fractional crystallization, partial melting of hydrothermally altered basaltic lava flows or intrusions, anatexis of old basement crust, or hybridization between basaltic and crustal melts. The Barda and Alech Hills, dominated by granophyre and rhyolite, respectively, form the largest silicic complexes in the Deccan Traps CFB province, India. We present petrographic, mineral chemical, and whole-rock geochemical (major and trace element and Sr-Nd isotopic) data

on rocks of both complexes, along with ^{40}Ar-^{39}Ar ages of 69.5-68.5 Ma on three Barda granophyres. Whereas silicic magmatism in the Deccan Traps typically postdates flood basalt sequences, the Barda granophyre intrusions (and the Deccan basalt flows they intrude) significantly predate (by 3-4 million years) the 66-65 Ma flood basalt outburst forming the bulk of the province. A tholeiitic dyke cutting the Barda granophyres contains quartzite xenoliths, the first being reported from Saurashtra and probably representing Precambrian basement crust. However, geochemical-isotopic data show little involvement of ancient basement crust in the genesis of the Barda-Alech silicic rocks. We conclude that these rocks formed by advanced fractional crystallization of basaltic magmas in crustal magma chambers. The sheer size of each complex (tens of kilometers in diameter) indicates a very large mafic magma chamber, and a wide, pronounced, circular-shaped gravity high and magnetic anomaly mapped over these complexes is arguably the geophysical signature of this solidified magma chamber. The voluminous silicic magmatism in the Barda and Alech complexes, derived by flood basalt fractionation, implies substantial crustal growth (as opposed to crustal reworking) during early Deccan CFB magmatism.

Keywords: Deccan Traps; Saurashtra; granophyre; rhyolite; Ar-Ar dating; petrogenesis

†Corresponding author: ciro.cucciniello@unina.it

1. Introduction

Silicic (granitic and rhyolitic) rocks are found in all continental flood basalt (CFB) provinces, sometimes in volumetrically significant amounts. Notable volumes of rhyolite,

for example, occur in the Karoo and Paraná CFB provinces (e.g. Cleverly, Betton & Bristow, 1984; Garland, Hawkesworth & Mantovani, 1995) and in the Snake River Plain "hotspot track" associated with the Columbia River CFB province (e.g. Ellis *et al*. 2013). The Deccan Traps CFB province of India, though poor in silicic rocks overall, has significant concentrations of these rocks in its western and northwestern parts, along the western Indian rifted margin. As in many other rifted-margin CFB provinces like the Karoo (Melluso *et al*. 2008), silicic magmatism in the Deccan generally postdates thick flood basalt sequences (e.g., Sheth & Melluso, 2008).

The Barda Hills (dominantly composed of granophyre) and Alech Hills (dominantly rhyolite) in Saurashtra, northwestern Deccan Traps, form the largest silicic complexes in the entire province (Fig. 1a, b). Each complex covers several tens of kilometers in diameter. Yet no focused study of the Barda complex exists since those by Dave (1971) and De & Bhattacharyya (1971), and almost no geological, petrological or geochemical information on the Alech complex is available in the otherwise vast Deccan Traps literature. The petrogenesis of silicic rocks in CFB provinces is a topic of considerable interest, and we have carried out a mineralogical and geochemical-isotopic study of select Barda-Alech silicic rocks to understand their petrogenetic evolution. We have also dated, by the $^{40}Ar/^{39}Ar$ incremental heating technique, three of the Barda granophyres. The combined results show that the silicic rocks are products of fractional crystallization of early basaltic magmas, with little or no input from pre-existing crust, and, in contrast to the general observation in CFB provinces, the Barda granophyre plutons distinctly predate the main (66-65 Ma) Deccan CFB eruptions. The results indicate crustal growth by early, flood basalt-derived silicic magmas in the Deccan Traps.

2. Geology

The large (present-day areal extent 500,000 km^2) Deccan Traps CFB province in west-central India is made up of flat-lying flood tholeiite lavas reaching a stratigraphic thickness of 3.5 km in the Western Ghats escarpment (Fig. 1a). The Saurashtra peninsula in the northwestern part of the Deccan province, also covered by the Deccan lavas, is nearly flat and low-lying, with few thick vertical sections through the lavas, and its coastal fringes covered by Tertiary or Quaternary limestones and alluvium. However, special features of Saurashtra's Deccan geology, noted for a long time, include several volcano-plutonic complexes (e.g. Fedden, 1984; Adye, 1914; Mathur, Dubey & Sharma, 1926; Auden, 1949), a great range of rock types including primitive picrites (e.g. Krishnan, 1926; Chatterjee, 1932; West, 1958; Krishnamacharlu, 1972; Krishnamurthy & Cox, 1977), and an abundance of rhyolite and granophyre (e.g. Subba Rao, 1971; Dave, 1971; De & Bhattacharyya, 1971; De, 1981). A large ring dyke of granophyre or silicic porphyry cuts the gabbro-diorite-monzonite plutonic complex of Mount Girnar (1117 m, Fig. 1b; Mathur, Dubey & Sharma, 1926). Osham Hill (314 m) to the northwest of Mount Girnar exposes flows of rhyolite and pitchstone capping tholeiitic flows; the silicic rocks show spectacular flow layering and flow folding and represent a rheomorphic, lava-like ignimbrite (Wakhaloo, 1967; Sheth *et al*. 2012).

The Barda Hills, near Porbandar town on the Arabian Sea and composed dominantly of granophyre, reach a substantial height of 627 m amsl (Fig. 2, 3a). There are many individual granophyre stocks emplaced through low-lying basaltic lava flows (Dave, 1971; De & Bhattacharyya, 1971). Barda granophyres generally form rounded and massive outcrops and are intruded by mafic dykes in the northern parts (e.g. BR4, Fig. 2). The peripheries of the Barda Hills are occupied by the Quaternary Miliolite Limestone

(e.g. Marathe, Rajaguru & Lele 1977) providing raw material for cement factories in the area.

In comparison, the Alech Hills, dominantly composed of rhyolites, form a series of low (~150-298 m amsl) and distinctly arcuate to concentric hill ranges whose intervening depressions are covered by Miliolite Limestone. Few exposed sections across these ranges are available. Misra (1981) has considered these arcuate hill ranges to represent ring dykes. However, we have observed a small outcrop of volcanic tuff 2 km north of Khageshri village, near the centre of the ring complex (Fig. 2). More suggestively, the rhyolite just east of Dhoriyo Nes hamlet (sample AL7, Fig. 2) shows large-scale flow layering and flow folding (Fig. 3b), and may be a rheomorphic, lava-like ignimbrite. If so, the Alech Hills rhyolites may represent large-scale ring-fracture lavas (including lava-like ignimbrites) like those of calderas of the Snake River Plain (e.g. Coble & Mahood, 2012). The Alech rhyolites are cut by dark-coloured silicic dykes such as AL4 and AL11 (Fig. 2).

3. Petrography

The Barda granophyres (samples BR1, 2, 3, 5, 6, 7, 8, 9, 10, 11, 12) are fine- to medium-grained rocks. They exhibit well-developed granophyric texture (Fig. 4a). Some of the samples are porphyritic (e.g. BR3). The rocks are made up of alkali feldspars (often perthitic, and generally making up 50-70% of the rock), quartz (subhedral to anhedral, making up 20-30% of most samples), minor plagioclase, and Fe-Ti oxides. Clinopyroxene grains have been observed in some samples (BR3, BR7, BR11, BR12; Fig.4b). Accessory minerals are zircon, baddeleyite, titanite and fluorite. De & Bhattacharyya (1971) observed Fe-rich olivine and ferroaugite in some of the granophyres.

Basalt and dolerite dykes in the Barda Hills, with phenocrysts of olivine, plagioclase (often forming glomeroporphyritic aggregates) and clinopyroxene set in a groundmass of plagioclase, clinopyroxene and glass, have been reported by Dave (1971). A basaltic andesite dyke exposed to the north of Ghumli village (Fig. 2; our sample BR4) consists of plagioclase phenocrysts set in a fine-grained groundmass with plagioclase, clinopyroxene, orthopyroxene, quartz, alkali feldspars and opaque oxides (Fig. 4c, d). Centimeter-size quartzite xenoliths containing quartz (mode 90%), plagioclase, orthopyroxene, alkali feldspars and magnetite (Fig. 4c, e) are found in the dyke BR4. They probably represent the unexposed Precambrian crustal basement of the Saurashtra region. They are the first reported case of basement xenoliths in Deccan Traps of Saurashtra, though zircon xenocrysts from Precambrian crust are known in some Rajula silicic dykes (Chatterjee *et al*. 2004).

De & Bhattacharyya (1971) reported monzodiorite (showing a hypidiomorphic texture with plagioclase, clinopyroxene, quartz, Fe-Ti oxides and apatite) ~3 km northwest of Sajanwala Nes (Fig. 2), and small dykes of aplite west of the Naliadhar Hills in the southern part of the Barda Hills (Fig. 2). The aplites consist of anhedral equigranular quartz and alkali feldspar (commonly in a micrographic intergrowth), opaque oxides, aegirine, and traces of riebeckite. Dave (1971) and De & Bhattacharyya (1971) also reported amphibole (riebeckite) in some Barda samples, though no primary hydrous phases are observed in our Barda (and Alech) rock samples.

The Alech rhyolites and dacites (samples AL1, 2, 4, 5, 7, 8, 9, 10, 11) are aphyric to weakly porphyritic (up to 10% phenocrysts). Alkali feldspar is a common phenocryst phase (Fig. 4f). Quartz occurs as phenocryst or microphenocryst in rhyolite AL9 with a fine-grained groundmass of quartz, alkali feldspars, magnetite, monazite and fluorocarbonates. Many Alech samples are visibly altered in hand specimen and under the

microscope; the alteration ranges from slight alteration of alkali feldspar phenocrysts to complete replacement of alkali feldspars and mesostasis by clay, zeolites, quartz, and calcite. Magnetite is partially replaced by red oxides or oxyhydroxides.

4. Mineral chemistry

4.1. Analytical methods

Seven rock samples from the Barda complex and nine from the Alech complex were chosen for mineral chemical analysis. Mineral compositions in the mafic rocks were determined at the University of Naples, using an Oxford Instruments Microanalysis Unit equipped with an INCA X-act detector and a JEOL JSM-5310 microscope in energy-dispersive spectrometry (EDS). The standard operating conditions included a primary beam voltage of 15 kV, filament current of 50-100 μA and variable spot size from 30,000 to 200,000x magnification, 20 mm WD. Measurements were made with an INCA X-stream pulse processor and with Energy software. Energy uses the XPP matrix correction scheme developed by Pouchou & Pichoir (1988), and the pulse pile-up correction. The quant optimization is carried out using cobalt (FWHM – full width at half maximum peak height – of the strobed zero = 60-65 eV). The following standards were used for calibration: diopside (Ca), San Carlos olivine (Mg), anorthoclase (Al, Si), albite (Na), rutile (Ti), fayalite (Fe), Cr_2O_3 (Cr), rhodonite (Mn), orthoclase (K), apatite (P), fluorite (F), barite (Ba), strontianite (Sr), zircon (Zr, Hf), synthetic Smithsonian orthophosphates (REE, Y, Sc), pure vanadium, niobium and tantalum (V, Nb, Ta), Corning glass (Th and U), sphalerite (S, Zn), galena (Pb), sodium chloride (Cl) and pollucite (Cs). The Kα, Lα, or Mα lines were used for calibration, according to the element. Backscattered electron

(BSE) images were obtained with the same instrument (Fig. 4b-f). The mineral analyses are reported in Tables 1-4, and plotted in Figure 5.

4.2. Results

Plagioclase in Barda granophyres ranges in composition from oligoclase ($An_{21-19}Ab_{72-74}Or_7$) to albite ($An_{11}Ab_{82}Or_7$). De & Bhattacharyya (1971) determined similar plagioclase phenocryst compositions of An_{15} to An_{21} from optic axial angle measurements. Unexsolved alkali feldspars in Barda granophyres range from sodic to potassic orthoclase ($An_1Ab_{62-7}Or_{37-92}$) (Table 1; Fig. 5a).

In basaltic andesite dyke BR4, plagioclase phenocrysts are bytownite ($An_{71-80}Ab_{27-20}Or_{1-0}$) whereas groundmass plagioclase ranges from labradorite ($An_{58}Ab_{39}Or_3$) to andesine ($An_{46-45}Ab_{49-51}Or_{5-4}$). Rare K-feldspar ($An_1Ab_{11}Or_{88}$) is found in the groundmass (Fig. 5a). Plagioclase in the basement xenoliths in the dyke BR4 ranges from labradorite ($An_{64}Ab_{35}Or_1$) to andesine ($An_{50-48}Ab_{47-49}Or_3$) and the xenoliths contain rare K-feldspar ($An_0Ab_6Or_{94}$).

Phenocrysts of alkali feldspar in the Alech rhyolites (AL2, AL4) are anorthoclase ($An_{12-3}Ab_{71-63}Or_{17-34}$) (Table 1; Fig. 5a). Groundmass alkali feldspars range from $An_2Ab_{60}Or_{38}$ to $An_1Ab_{50}Or_{49}$. Sanidine occurs in the groundmass of Alech rhyolites AL8 and AL9 (Fig. 5a).

Pyroxenes in Barda granophyres (Table 2) are hedenbergite ($Ca_{43-46}Mg_0Fe_{57-54}$; Mg# = Mg*100/(Mg+Fe_t) = 0) and aegirine-augite (Na_2O = 1.8-4.6 wt.%; Mg# = 0) typical of alkaline rocks (Fig. 5b). De & Bhattacharyya (1971) reported similar compositions. TiO_2 is generally low (0-0.8 wt.%) and tends to decrease with decreasing FeO content of the clinopyroxene. In the basaltic andesite dyke BR4, augite ($Ca_{43-41}Mg_{41-44}Fe_{16-15}$; Mg# =

73-75) and orthopyroxene ($Ca_{2-3}Mg_{65-66}Fe_{31-32}$; Mg# = 67-69) are the two pyroxenes (Fig. 5b). Orthopyroxene with similar composition ($Ca_{2-3}Mg_{66-67}Fe_{31-32}$) is observed in the basement xenoliths of dyke BR4. Equilibration temperatures based on clinopyroxene-liquid geothermometer (Putirka, 2008) range from 1003 to 1043 °C. Two-pyroxene geothermometry (Putirka, 2008) yields values close to 900 °C.

Titaniferous magnetite in the Barda granophyres has variable TiO_2 (1.0-24.4 wt.%; 3-69 mol.% ulvöspinel) and low Al_2O_3 (<0.7 wt.%) contents (Table 3). In dyke BR4 the titaniferous magnetite has low ulvöspinel (11-26 mol.%) contents. Ilmenite has a limited range of solid solution with haematite (ilmenite from 85 to 95 mol.%). MgO ranges from 1.2 to 2.4 wt.% in ilmenites in dyke BR4. Equilibrium magnetite-ilmenite pairs in Barda granophyres and basaltic andesite yield temperature and log fO_2 of 583-750 °C and –14 to –20, respectively (calculated using the ILMAT program of Lepage, 2003), indicating late-stage subsolidus reequilibration.Zircon and titanite are ubiquitous as euhedral, prismatic microcrystals in the Barda granophyres and show a homogeneous major element composition. Zircon contains up to 2.4 wt.% HfO_2 (Table 4). Monazite-(Ce) has been observed as accessory phase in the Alech rhyolite AL9. It contains La_2O_3 in the range 15.1–20.3 wt.% and Ce_2O_3 from 34.0 to 42.6 wt.%. Thorium concentration ranges from 1.1 to 7.4 wt.% ThO_2 (Table 4).

5. $^{40}Ar/^{39}Ar$ dating

Three whole-rock samples of the Barda granophyres were dated by the $^{40}Ar/^{39}Ar$ incremental heating technique. Samples BR3 and BR5 were collected from low-lying outcrops on the Ranavav-Bhanvad road, north and south of Sajanwala Nes and Hanumangadh, respectively (Fig. 2). Sample BR12 was taken from the base of a jointed

granophyre hillock north of Ranavav Railway Station (Fig. 2). None of the Alech rocks were suitable for $^{40}Ar/^{39}Ar$ dating because of their significant alteration.

5.1. Analytical methods

Fresh rock chips were crushed, sieved, and cleaned in deionized water in an ultrasonic bath. About 0.02 g of each was packed in aluminium capsules. Minnesota hornblende (MMhb-1, age 523.1 ± 2.6 Ma, Renne *et al*. 1998) and high-purity CaF_2 and K_2SO_4 salts were used as monitor samples. High-purity nickel wires were placed in both sample and monitor capsules to monitor the neutron fluence variation, which was typically ~5%. The aluminium capsules were kept in a 0.5 mm thick cadmium cylinder and irradiated in the heavy water-moderated DHRUVA reactor at the Bhabha Atomic Research Centre (BARC), Mumbai, for ~100 h. The irradiated samples were repacked in aluminium foil and loaded on the extraction unit of a Thermo Fisher Scientific noble gas preparation system. Argon was extracted in a series of steps up to 1400 ^{o}C in an electrically heated ultrahigh vacuum furnace. The argon released in each step, after purification using Ti-Zr getters, was analyzed with a Thermo Fisher ARGUS VI mass spectrometer, located at the National Facility for ^{40}Ar-^{39}Ar Geo-thermochronology in the Department of Earth Sciences, IIT Bombay. The mass spectrometer is equipped with five Faraday cups fitted with 10^{11} Ω resistors.

Interference corrections for Ca- and K-produced Ar isotopes based on analysis of CaF_2 and K_2SO_4 salts were $(^{36}Ar/^{37}Ar)_{Ca}$, $(^{39}Ar/^{37}Ar)_{Ca}$ and $(^{40}Ar/^{39}Ar)_{K}$ = 0.000471, 0.001145 and 0.006842, respectively. ^{40}Ar blank contributions were 1-2% or less for all temperature steps. The irradiation parameter *J* for each sample was corrected for neutron flux variation using the activity of nickel wires irradiated with each sample. Values of

fluence-corrected *J* for various samples are as follows: BR3, 0.000480 ± 0.000002; BR5, 0.000490 ± 0.000002; BR7, 0.000487 ± 0.000002; BR12, 0.000516 ± 0.000003. The plateau ages reported comprise a minimum of 50% of the total ^{39}Ar released and four or more successive degassing steps whose mean ages overlap at the 2σ level excluding the error contribution (0.5%) from the *J* value. The data were plotted using the program Isoplot/Ex v. 3.75 (Ludwig, 2012).

5.2. Results

Table 5 gives the summary of the ^{40}Ar/^{39}Ar dating results (plateau, isochron and inverse isochron ages with 2σ uncertainties) for the three Barda granophyre samples. Plateau spectra and isochron plots for the three samples are shown in Figure 6. The full, stepwise analytical data are given in supplementary Table S1.

Granophyre BR3 yielded an 11-step plateau constituting as much as 89.4% of the total ^{39}Ar release, and an age of 68.5 ± 0.4 Ma (2σ) (Fig. 6a). Granophyre BR5 yielded a 12-step plateau constituting 81.3% of the ^{39}Ar release, and an age of 69.9 ± 0.3 (2σ) (Fig. 6b). Granophyre BR12 yielded 7-step plateau constituting 67.1% of the ^{39}Ar release, and an age of 69.0 ± 0.5 (2σ) (Fig. 6c). All three samples have isochron ages and inverse isochron ages which are statistically indistinguishable from the plateau ages (Fig. 6a-c, Table 5). The isochrons and inverse isochrons also have acceptable MSWD values and intercepts showing atmospheric values (295.5) of the trapped ^{40}Ar/^{36}Ar ratio, which suggests, along with the well-developed plateau spectra for all samples, that these ages are true crystallization ages. We take the plateau ages of the three granophyre samples to represent their intrusion and crystallization ages.

6. Geochemistry

6.1. Analytical methods

The seven rock samples from the Barda complex and nine from the Alech complex analyzed for mineral chemical data were also analyzed for whole-rock major and trace element (including rare earth element) data at Actlabs (Canada). Rock powders were mixed with fluxes lithium metaborate and lithium tetraborate and fused in an induction furnace. The molten samples were immediately poured into a solution of 5% nitric acid containing an internal standard and mixed continuously until completely dissolved (~30 min). The samples were analyzed for major oxides and selected trace elements (Ba, Be, Sc, Sr, V, Y and Zr) on a combination simultaneous/sequential Thermo Jarrell-Ash ENVIRO II ICP or a Varian Vista 735 ICP. Calibration was performed using seven USGS and CANMET certified reference materials. One of the seven standards was used during the analysis for every group of ten samples. The fused sample solutions were diluted and analyzed by a Perkin Elmer Sciex ELAN 6000, 6100 or 9000 ICP/MS for other trace elements (Cr, Co, Ni, Cu, Zn, Ga, Ge, As, Rb, Nb, Mo, Sn, Cs, La, Ce, Pr, Nd, Sm, Eu, Gd, Tb, Dy, Ho, Er, Tm, Yb, Lu, Hf, Ta, W, Pb, Bi, Th and U). Three blanks and five control samples (three before the sample group and two after) were analyzed per group of samples. Duplicates were fused and analyzed after every 15 samples. Analyses of international standards are reported in Table 6. The weight loss on ignition was obtained with gravimetric techniques, firing at 1000°C small aliquots of powders previously dried at 110°C overnight. Major and trace element (including the rare earth element) data for the Barda-Alech rocks are presented in Table 6.

Sr-Nd isotopic analyses were performed on 12 samples (six Barda granophyres, Barda basaltic andesite dyke BR4, and five Alech rhyolitic rocks), using a fully automatic Thermo Fisher TRITON multicollector thermal ionization mass spectrometer (TIMS), located at the National Facility for Isotope Geology and Geochronology, Indian Institute of Technology Roorkee. Sample dissolution procedures and other analytical details are as described by Sheth *et al*. (2011, 2012). The Sr-Nd isotopic data are reported in Table 7.

6.2. Alteration effects

Like hand specimen and petrographic observations, LOI values indicate that several samples (in particular the Alech rocks; e.g. AL3, 5, 10, 11) are altered. LOI values range from 0.30 to 1.64 wt.% for Barda rock samples and from 1.10 to 5.51 wt.% for Alech rock samples. The extremely high SiO_2 content in some Alech rhyolites (e.g. 86.71 wt.% in AL3) indicates silicification processes mostly associated with alkali mobility. Alteration also appears to have variably affected K, Na, Rb, and Ba contents in the Alech samples, as noted from poor correlations between K, Na, Rb, and Ba and more alteration-resistant elements such as Zr or Nb. We therefore do not use Rb, Ba, K and Na data in this study and use only the alteration-resistant elements (Ti, Zr, Nb, Y, Th, and REE) and their ratios for geochemical interpretations.

6.3. Results

We used the SINCLAS program of Verma, Torres-Alvarado & Sotelo-Rodriguez (2002) to recalculate the major oxide data on an LOI-free basis and to obtain rock names recommended by the IUGS Sub-commission on the Systematics of Igneous Rocks based

on the total alkalis-silica diagram (Le Bas *et al*. 1986). As given by SINCLAS, all Barda granophyres are of rhyolite composition, whereas the dyke BR4 is a basaltic andesite. Most Alech samples are also of rhyolite composition, including dyke AL4, but sample AL07 from the outcrop with flow folding (Fig. 3b) and dyke AL11 from Chek Hill are dacites. The basaltic andesite dyke BR4 has 7 wt.% normative quartz (supplementary Table S2).

The Barda granophyres are mainly metaluminous (A/CNK = mol $Al_2O_3/(CaO+Na_2O+K_2O)$ = 0.88-0.93). They are chemically uniform, with SiO_2 ranging from 70.2 to 72.9 wt.%, TiO_2 0.3-0.5 wt.%, Al_2O_3 11.6-12.7 wt.% and Fe_2O_{3t} 4.4-5.8 wt.%. All samples contain very low MgO contents (0.1-0.2 wt.%). Their alteration-resistant trace elements also have narrow ranges of concentration (Zr = 447-557 ppm, Nb = 49-55 ppm, Y = 87-112 ppm) and ratios of concentrations (Zr/Nb = 9-10, Y/Nb = 1.7-2.3). The values of these ratios are not too different from those of mantle-derived mafic melts with slightly enriched composition and are similar to those of various Deccan (particularly Saurashtra) mafic lavas and dykes (Zr/Nb = 5-26; Y/Nb = 1-9; Cucciniello *et al*. 2015 and references therein).

The Barda granophyres show low to moderate light- to heavy rare earth element (REE) fractionation in chondrite-normalized patterns (La_n/Yb_n = 2.7-4.5; the subscript 'n' means chondrite-normalized; Fig. 7a). All granophyres show distinct negative Eu anomalies, with Eu_n/Eu^* = 0.5-0.7, where $Eu^* = (Sm_n + Gd_n)/2$. Basaltic andesite BR4 has lower REE contents than the granophyres and has a small negative Eu anomaly (Eu/Eu* = 0.8) in its chondrite-normalized REE pattern (Fig. 7a). In primitive mantle-normalized multielement patterns (Fig. 7b) the Barda granophyres show small or no troughs at Nb and marked troughs at Sr and Ti. The basaltic andesite BR4 shows negative Nb, Sr and Ti anomalies in its pattern.

The fresher (LOI < 3.4 wt.%) of the Alech rhyolites and dacites (AL1, 4, 7, 8, 9; SiO_2 = 66.5-72.6 wt.%) are weakly peraluminous, with A/CNK = 0.98-1.14 and low (0.3 wt.%) to no normative corundum in the CIPW norm (supplementary Table S2). They can be divided into two groups. The first group (samples AL5, 7, 8, 10, 11) is characterized by low Nb (20-27 ppm) and moderate Zr (282-384 ppm) and Y (43-73 ppm) contents. These rocks are slightly enriched in LREE, with La_n/Yb_n ranging from 3.7 to 4.1. Their REE patterns are relatively flat in the middle and heavy REE portions of the pattern (Fig. 8a), with $Gd_n/Lu_n \approx 0.8$-1.0. Negative Eu anomalies (Eu/Eu* = 0.6-0.7) are present in the chondrite-normalized REE patterns of this group, and their mantle-normalized incompatible element patterns display troughs at Nb, Sr and Ti (Fig. 8a). The second group (samples AL1, 3, 4, 9) shows significant enrichments in the incompatible elements compared to the first group, with high Nb (108-852 ppm), Zr (584-2650 ppm) and Y (89-291 ppm) concentrations. Their chondrite-normalized patterns are characterized by moderate enrichment in LREE (La_n/Yb_n = 4.3-5.7), a very flat HREE pattern, and negative Eu anomalies, with the lowest value of Eu/Eu* (0.04) found in the rhyolite AL09 (Fig. 8b). In their mantle-normalized multielement patterns (Fig. 8b), this group shows troughs at Sr and Ti.

Samples AL8 and AL9 were taken from adjacent rhyolite dykes just south of Dhoriyo Nes hamlet (Fig. 2). At Dhoriyo Nes, Maithani *et al*. (1996) have described a few rhyolite dykes with strong enrichments in Nb (up to 1000 ppm), Zr (>1000 ppm) and Y (up to 337 ppm). Our dyke AL9 (852 ppm Nb, 2650 ppm Zr, 291 ppm Y) undoubtedly represents one of them. The associated dyke AL8 does not show these notable Nb-Zr-Y enrichments.

Measured Sr-Nd isotopic ratios of the 12 analyzed Barda-Alech rocks have been recalculated as initial ratios at 65 Ma (Table 7, Fig. 9). Six Barda granophyres show a

restricted range of $(^{87}Sr/^{86}Sr)_t$ from 0.705987 to 0.706176. Their $(^{143}Nd/^{144}Nd)_t$ values range from 0.512555 ($\varepsilon_{Nd}t$ = 0.0) to 0.512614 ($\varepsilon_{Nd}t$ = +1.1). The Barda basaltic andesite dyke BR4 has the highest $(^{87}Sr/^{86}Sr)_t$ of 0.707392 and lowest $(^{143}Nd/^{144}Nd)_t$ of 0.510996 ($\varepsilon_{Nd}t$ = –30.4) of all analyzed samples. Alech rocks of the first group described above (here represented by samples AL5, 7, 10, 11) have more radiogenic $(^{87}Sr/^{86}Sr)_t$ (0.706361-0.707379), and less radiogenic $(^{143}Nd/^{144}Nd)_t$ (0.512485 to 0.512517, $\varepsilon_{Nd}t$ = –1.4 to –0.7), compared to those of the second group (here represented by a single sample AL4) which has $(^{87}Sr/^{86}Sr)_t$ = 0.705894 and $(^{143}Nd/^{144}Nd)_t$ = 0.512655; $\varepsilon_{Nd}t$ = +2.0) and the Barda granophyres (Fig. 9).

Samples AL10 and AL11 have identical $(^{87}Sr/^{86}Sr)_t$ and $(^{143}Nd/^{144}Nd)_t$ isotopic ratios (Table 6, Fig. 9). AL10 is the tuffaceous-looking rhyolite (possibly also an ignimbrite) forming Check Hill (226 m, Fig. 2) and AL11 is a dark grey, very fine-grained dyke cutting AL11. Both samples are visibly altered and have high LOI values (4.94 and 4.83 wt.%, respectively). They have very similar Th, Nb, Zr, Hf, Ti and REE contents, as shown by their almost overlapping primitive mantle-normalized patterns in Figure 8c, but differ considerably in Rb, Ba, K and Na, the fluid-mobile elements. The isotopic and trace element data indicate that rhyolite AL10 and the dacite dyke AL11 cutting it (*not* a feeder) were both derived from the same magma reservoir.

7. Discussion

7.1. Emplacement ages

The ^{40}Ar-^{39}Ar data obtained in this study, and field relationships (Dave, 1971; De & Bhattacharyya, 1971) imply that the Barda granophyre plutons were emplaced at 69.5-68.5

Ma into Deccan basalt flows. The granophyre plutons and the local basalts thus significantly predate the massive 66-65 Ma Deccan flood basalt outburst in the Western Ghats as well as the northern Deccan region including Mount Pavagadh (Baksi, 2014; Schoene *et al*. 2015; Parisio *et al*. 2016). Generally, in widely separated areas of the Deccan province, field relationships (and ^{40}Ar-^{39}Ar data) show silicic lavas and intrusions to have been emplaced after thick flood basalt sequences. The best examples are Mount Pavagadh (Chatterjee, 1961; Sheth & Melluso, 2008; Parisio *et al*. 2016), Osham Hill (Wakhaloo, 1967; Sheth *et al*. 2012), and Mumbai (Sheth & Pande, 2014). In other flood basalt provinces of the world (such as the Karoo) also, rhyolitic lavas and ignimbrites have generally erupted towards the close or at the end of the flood basalt volcanism (e.g. Melluso *et al*. 2008). The early silicic magmatism in the northwestern Deccan Traps, represented by the Barda granophyre plutonism, is therefore a novel result of this study.

We have not dated any of the Alech rocks because of their generally weathered nature, and therefore we do not know the age of emplacement of the complex relative to the main tholeiitic phase in the Deccan province at 66-65 Ma. However, the Alech complex, like the Barda complex, postdates the local Deccan basalt flows.

7.2. Petrogenesis

Silicic igneous rocks are common in intraplate extensional settings such as the Basin and Range province (e.g. Colgan *et al*. 2006), post-collisional extensional settings (e.g. Nedelec, Stephens & Fallick 1995), and at rifted continental margins associated with CFB volcanism (e.g. Melluso *et al*. 2001, 2008; Cucciniello *et al*. 2010), and provide important information on tectonic deformation and the generation, storage and transport of silicic magma in the continental lithosphere. Silicic rocks in general, and those in CFB provinces

in particular, are known to be produced by several mechanisms, such as advanced fractional crystallization of mafic magmas (e.g. Soesoo, 2000; Turner, Foden & Morrison, 1992; Melluso *et al*. 2008; McCurry *et al*. 2008), crustal assimilation with fractional crystallization (AFC) (e.g. Sheth & Melluso, 2008; Cucciniello *et al*. 2010), hybridization between mantle-derived and crustally derived magmas (e.g. Wikham *et al*. 1996), partial melting of hydrothermally altered basic lavas or intrusions (e.g. Zellmer *et al*. 2008; Colón *et al*. 2015), and anatexis of old basement crust (e.g. Riley *et al*. 2001; Shellnutt *et al*. 2012; Zhu *et al*. 2017).

The data presented in this study show that the Barda granophyres, mainly metaluminous have high Fe Number [0.95-0.98; Fe# = $FeO_t/(FeO_t+MgO)$], Ga/Al (3.1-3.3) ratios, Zr, Nb and REE contents (Table 1). These geochemical characteristics (Ga/Al = 3.75; Zr = 528 ppm; Nb = 37 ppm) resemble A-type (ferroan) granitoids typical of within-plate settings (e.g. Whalen, Currie & Chappell, 1987). Similarly, the Alech rhyolites and dacites have geochemical features typical of silicic rocks of within-plate settings (e.g. Fe# = 0.81-0.99; Ga/Al = 2.6-5.5).

Direct derivation of the Barda-Alech silicic rocks by partial melting of old crustal rocks (e.g. western Indian Precambrian granites) is precluded by the Sr-Nd isotopic data, because these ancient granites have much higher $^{87}Sr/^{86}Sr$ ratios (e.g. 0.7690, Gopalan *et al*. 1979) than the Barda-Alech silicic rocks. It is only the Barda basaltic andesite dyke BR4 which has a very unradiogenic Nd isotopic composition ($\varepsilon_{Nd}t$ = –30.4) similar to some ancient Indian granites (e.g. Jayananda *et al*. 2006). This simply reflects the incorporation of old basement crust in the dyke magma, possibly the same crust whose quartzitic xenoliths are still found in this dyke.

Basic amphibolites, in the presence of a free fluid phase, produce relatively silicic (tonalitic or trondhjemitic) partial melts over a wide melting range (5-30 kb, 750-1100 °C,

e.g. Winther & Newton, 1991; van der Laan & Wyllie, 1991; cited in Peng *et al*. 1994). However, Archaean basic amphibolites analyzed from Rajasthan, northwestern India, have average $^{87}Sr/^{86}Sr$ of 0.7151 and ε_{Nd} of –12 (Gopalan *et al*. 1990), very unlike those of the Barda-Alech silicic rocks.

The absence of primary minerals such as muscovite, cordierite, garnet, aluminosilicates (andalusite or sillimanite) and tourmaline in the Barda-Alech rocks (and the presence of aegirine-augite in the Barda granophyres) also excludes an origin for these rocks as anatectic melts of metasedimentary protoliths. In addition, the Barda-Alech rocks have Zr and Y contents much higher than those normally observed in anatectic, S-type leucogranites from pelitic sources worldwide (e.g. Whalen, Currie & Chappell, 1987; Bea, Pereira & Stroh, 1994).

Silicic magmas derived from partial melting of garnet granulites (e.g. Verma, 1999) or eclogites are characterized by low Y and HREE contents as consequence of residual garnet (Schnetger, 1994). The high Y (>43 ppm) and HREE (e.g. Yb_n >17) contents observed in the Barda-Alech silicic rocks thus rule out garnet granulite or eclogite sources.

Partial melting of previously emplaced basaltic rocks or gabbroic intrusions, likely hydrothermally altered, is also a plausible hypothesis for the genesis of silicic magmas. This mechanism can explain the absence of compositions intermediate between basalts and granophyres-rhyolites-dacites and the mantle-like Sr-Nd isotopic ratios of the Barda-Alech silicic rocks. However, experimental work shows that water-saturated melting of basaltic rocks amphibolites and greenstones at 1, 3, 6.9 and 10 kbar pressure (Helz, 1976; Spulber & Rutherford, 1983; Beard & Lofgren, 1991; Wolf & Wyllie, 1994) should produce liquids with higher Al_2O_3 and CaO contents and lower K_2O contents than the Barda-Alech silicic rocks (Fig. 10). We were unable to reproduce the geochemical characteristics of the

Barda-Alech silicic rocks by partial melting (assuming a volatile-free source) of basaltic andesite BR4 composition (or Osham basaltic andesite OSH5 composition, Sheth *et al*. 2012) with no subsequent fractionation (Fig. 11). Partial melting models using other Deccan basalt compositions from Saurashtra (Melluso *et al*. 1995) also fail to reproduce the geochemical characteristics of the Barda-Alech silicic rocks (Fig. 11).

The small range of Sr-Nd isotopic variation within the Barda granophyres ($(^{87}Sr/^{86}Sr)_t$ = 0.705988-0.706066, $\varepsilon_{Nd}t$ = 0.0 to +1.1) does not permit significant open-system processes and crustal incorporation within the Barda granophyres. The slight positive correlation between $(^{143}Nd/^{144}Nd)_t$ and Nd concentrations, and the absence of Pb peaks and Nb troughs in mantle-normalized incompatible element patterns (Fig. 7b, 8b), also indicates that assimilation of crustal material was negligible in the genesis of the Barda granophyres and Alech samples AL1, 3, 4, 9 (group 2). Crustal contamination may have had some role in the genesis of the Alech samples AL5, 7, 8, 10, 11 (group 1) which have higher $(^{87}Sr/^{86}Sr)_t$ of 0.706361-0.707379 and comparatively lower $\varepsilon_{Nd}t$ values (–0.7 to –1.4), with Nb troughs in mantle-normalized incompatible element patterns.

We therefore suggest that a model of advanced, nearly-closed system fractional crystallization of early basaltic melts, stored in crustal magma chambers, can explain the production of the Barda-Alech silicic rocks. Trace element abundance patterns provide convincing evidence for derivation of the Barda granophyres and Alech rhyolites by fractional crystallization of basalt. Negative anomalies of Ba, Sr and Eu in the mantle-normalized multielement patterns of the silicic rocks are suggestive of fractionation of plagioclase feldspar, whereas negative Ti anomalies suggest fractionation of Ti-bearing oxides (Fig. 7b, 8b). Simulation of fractional crystallization paths (Fig. 11) starting from the Osham basaltic andesite OSH5 (Sheth *et al*. 2012) and the Barda basaltic andesite BR4

indicates that the Barda-Alech silicic rocks could be the result of nearly-closed system fractional crystallization (90-95%) of a low-Ti basaltic magma.

The depth at which Barda-Alech silicic magmas were stored, prior to shallower-level intrusion or extrusion, is difficult to assess, as the mineral assemblage is not suitable for geobarometry. However, the presence of a small amount of primary amphibole in some of the Barda silicic rocks (Dave, 1971; De & Bhattacharyya, 1971) indicates that the crystallizing magmas were hydrous. A semiquantitative estimate of the pressure of equilibration can be obtained using the synthetic system quartz-albite-orthoclase-H_2O (Fig. 12). The Barda granophyres plot close to the water-saturated minimum compositions at 2 kbar and 3 kbar. Pressures for the Alech magmas range from 1 atm to 5 kbar, with the majority values at the shallower end.

Residual rhyolitic melt forming by closed-system fractional crystallization of basalt represents a very small percentage of original liquid (e.g. Bowen, 1928; McCurry *et al*. 2008). Whitaker *et al*. (2008) find that potassic rhyolitic melts can form by very advanced (96-97%) closed-system fractional crystallization of olivine tholeiite melts with 10.6 wt.% MgO. Many occurrences of small volumes of interstitial granophyric or rhyolitic melts are known from Deccan tholeiitic dykes and sills (e.g. Subba Rao, 1971; Sen, 1980). What is surprising therefore is the sheer volume of granophyre and rhyolite magma which is concentrated in the Barda and Alech complexes. The derivation of so much silicic magma by near-closed-system fractional crystallization requires a very large basaltic magma chamber in the crust beneath Saurashtra. Interestingly, the Barda and Alech complexes sit atop a pronounced, wide and roughly circular-shaped gravity high and magnetic anomaly (Chandrasekhar *et al*. 2002), which may indicate just such a mafic magma chamber, with ultramafic cumulates, in the upper crust (or several smaller, coalesced magma chambers). The Barda-Alech silicic rocks are thus the residual melts from advanced fractional

crystallization in this large mafic magma chamber. The monzodiorite reported from Sajanwala Nes (De & Bhattacharyya, 1971) may represent an intermediate-stage product of the same process. Also, such a large chamber may also have produced substantial crustal heating and melting. Our present sampling is necessarily limited, and it is probable that future intensive sampling of the Barda and Alech complexes, including in the high peaks of the former, may reveal many individual plutons or lavas with a substantial crustal input.

.

7.3. Genesis of silicic rocks of the Deccan Traps

Zhu *et al*. (2017) note the co-existence of mantle-derived and crustally-derived silicic magmas in parts of the Late Permian (260 Ma) Emeishan CFB province of China. Similarly, geochemical-isotopic data available for hitherto analyzed silicic rocks of the Deccan Traps (Fig. 9) indicate a combination of these processes, sometimes even for a single rock suite (e.g. Subba Rao, 1971; Chatterjee & Bhattacharji, 2001; Sheth & Melluso, 2008; Sheth *et al*. 2011, 2012), as follows:

(i) Advanced fractional crystallization of basaltic magmas: The best example of this mechanism in the Deccan, involving little crustal interaction, is the Barda-Alech silicic rocks of the present study. Some Chogat-Chamardi silicic rocks also appear to have formed in this way (Sheth *et al*. 2011). Potassic rhyolites of Rajpipla (Krishnamurthy & Cox, 1980), one of which has been analyzed for Sr-Nd isotopic composition (Mahoney *et al*. 1985), are also suitable candidates, as is a rhyolite from Tavidar in Rajasthan (Sen *et al*. 2012).

(ii) Assimilation and fractional crystallization (AFC): In this process, progressively more fractionated melts are more crustally contaminated, as commonly observed in mafic-

felsic suites. At Skye in the British Palaeogene igneous province, the granophyres have $(^{87}Sr/^{86}Sr)_t$ of 0.708-0.716, higher than for associated gabbros (0.703-0.709) (Moorbath & Bell, 1965). Similarly, granophyres in the Skaergaard Intrusion in East Greenland have higher Sr isotopic ratios than the bulk of the gabbros forming the intrusion (Leeman & Dasch, 1978). Silicic rocks in the Chogat-Chamardi complex are also much more contaminated than the gabbros and have been explained by AFC processes involving mafic magmas and old basement crust (Sheth *et al*. 2011). The Mount Pavagadh dacites and rhyolites have relatively high Zr (458-536 ppm), Nb (45-60 ppm) and Y (63-112 ppm) contents and are LREE-enriched (La_n/Yb_n = 7.2-11.5), and their $(^{87}Sr/^{86}Sr)_t$ varies from 0.70369 to 0.70826 (Sheth & Melluso, 2008). These authors modelled the silicic rocks by AFC involving a starting picritic magma and old felsic crust.

(iii) Partial melting of hydrothermally altered basic lavas or intrusions: Lightfoot, Hawkesworth & Sethna (1987) proposed that Mumbai rhyolites, with high incompatible trace element contents (e.g. Zr = 1509-1801 ppm; Nb = 260-319 ppm; Y = 143-177 ppm), low $(^{87}Sr/^{86}Sr)_t$ (0.7037-0.7074) and slightly negative $\varepsilon_{Nd}t$ (–0.5 to –1.3) were derived by partial melting of basaltic intrusions in the crust due to heating by other intrusions (or by fractional crystallization of basaltic melts). The Osham Hill silicic lavas (Sheth *et al*. 2012) have low TiO_2 (0.12-0.10 wt.%) and relatively high Zr (410-437 ppm) and Y (136-148 ppm) contents. They are LREE-enriched, with La_n/Yb_n ranging from 7.9 to 8.6. The Osham rhyolites have $\varepsilon_{Nd}t$ = –3.1 to –6.5, and $(^{87}Sr/^{86}Sr)_t$ values from 0.70709 to 0.70927. Notably, these silicic lavas have the same Al_2O_3 contents as the underlying mafic flows, and therefore Sheth *et al*. (2012) considered an origin by fractional crystallization of mafic melts (i.e. involving substantial plagioclase) untenable. They suggested an origin of the Osham silicic lavas by partial melting of hydrothermally altered and K-metasomatized

basaltic lavas or crustal intrusions, as proposed for some Icelandic rhyolites (Zellmer *et al*. 2008).

(iv) Anatexis of old basement crust: A role for anatexis of ancient basement crust in the genesis of Deccan silicic magmas, as advocated by Subba Rao (1971), appears valid for some of the Rajula rhyolites (Chatterjee & Bhattacharji, 2001; Chatterjee *et al*. 2004). It also seems valid for several of the Chogat-Chamardi granophyres and rhyolites (Sheth *et al*. 2011), which have TiO_2 in the range 0.26-1.1 wt.% and moderate to high Zr (373-1209 ppm) and Y (69-117 ppm) contents, and are LREE enriched, with La_n/Yb_n of 3.0-5.0. Their $(^{87}Sr/^{86}Sr)_t$ ratios are higher than 0.7275 and $\varepsilon_{Nd}t$ values range from +0.6 and –3.0 (Chamardi granophyres) to as low as –12.4 and –13.9 (Chogat rhyolites). The Tavidar rhyolite Tav07 may owe its very high $(^{87}Sr/^{86}Sr)_t$ to weathering, however (Sen *et al*. 2012).

Considered as a whole, Sr isotopic data for the Deccan silicic rocks hitherto available show a large gap, from about 0.7095 to 0.7275 (Fig. 9), separating those with little or no crustal input and those with very strong crustal input or of entirely crustal derivation. Nd isotopic compositions of the rocks show much greater continuity than Sr isotopic compositions.

8. Conclusions

The Barda and Alech complexes in the Saurashtra region are the largest silicic complexes in the Deccan CFB province, India. The Barda complex is mainly composed of coalescing granophyre plutons. The Alech complex is made up dominantly of rhyolite and dacite which are probably ring-fracture lavas and lava-like ignimbrites. Despite early studies (Adye, 1914; Dave, 1971; De & Bhattacharyya, 1971), neither complex has received much study by modern geoanalytical methods.

In this study we have provided basic geological information on both complexes, which we hope to substantially expand on in the future. We have also provided petrographic and mineral chemical data and whole-rock geochemical (major and trace element and Sr-Nd isotopic) data, and ^{40}Ar-^{39}Ar ages of three Barda granophyres. These ages indicate that the Barda granophyre intrusions are 69.5-68.5 Ma in age, and they and the Deccan basalt flows they intrude are thus significantly older (by 3-4 million years) than the main Deccan flood basalt outburst at 66-65 Ma in the Western Ghats and the northern Deccan regions (Baksi, 2014; Renne *et al*. 2015; Parisio *et al*. 2016). Whereas silicic magmatism (lava flows and intrusions) typically postdates thick sequences of flood basalts in the Deccan Traps, as well as in other CFB provinces of the world, the early silicic magmatism represented by the Barda granophyre plutonism is a novel result of considerable interest. It also indicates that the total duration of Deccan magmatism was no less than 8 million years (see e.g. Sheth & Pande, 2014 and references therein).

Though xenoliths of probable basement crust (the only known so far from Saurashtra) are present in a basaltic andesite dyke cutting the Barda granophyres, geochemical-isotopic data show little involvement of ancient basement crust in the genesis of the Barda-Alech silicic rocks. These data show that partial melting of several types of old basement lithologies (Indian Precambrian granitoids, amphibolites, metasedimentary rocks, garnetiferous granulites or granites), or partial melting of Deccan-age basaltic lavas or gabbro intrusions (possibly hydrothermally altered) within the Saurashtra crust, cannot have produced the Barda-Alech silicic rocks.

On the other hand, the geochemical-isotopic data indicate derivation of the Barda-Alech silicic rocks by prolonged, nearly closed-system fractional crystallization from low-Ti basaltic magmas stored in magma chambers located in the upper or middle crust. From the size of the Barda and Alech complexes (each tens of kilometers in diameter), a very

large mafic magma chamber is indicated, and is reflected in the pronounced, circular-shaped gravity high and magnetic anomaly mapped over these complexes (Chandrasekhar *et al*. 2002).

The voluminous, basalt fractionation-derived silicic magmatism in the Barda and Alech complexes implies substantial crustal growth (as opposed to crustal reworking) at an early stage of Deccan CFB magmatism.

Acknowledgements

Field work was supported by the Industrial Research and Consultancy Centre (IRCC, IIT Bombay) grant 09YIA001 to Sheth. Many thanks to Sergio Bravi for the preparation of thin sections and to Roberto de' Gennaro for his assistance in microprobe work. Funds for EPMA and whole-rock analyses by Cucciniello were provided Italian MIUR (PRIN 2015, 20158A9CBM to L. Melluso) and Fondi Ricerca di Ateneo (DR_3450_2016 to C. Cucciniello). Pande acknowledges Grant No. IR/S4/ESF-04/2003 from the Department of Science and Technology (Govt. of India) towards the development of the IIT Bombay-DST National Facility for ^{40}Ar–^{39}Ar Geo-thermochronology. He also thanks the IRCC, IIT Bombay, for maintenance support to the Facility (grant no. 15IRCCCF04). We thank Nilanjan Chatterjee for helpful comments on an earlier version of this work.

References

ADYE, E. H. 1914. *Economic Geology of the Nawanagar State in the Province of Kathiawar, India*. Thacker and Company, Mumbai, 262 p.

AUDEN, J. B. 1949. Dykes in western India – A discussion of their relationships with the Deccan Traps. *Transactions of National Academy of Sciences of India* **3**, 123–157.

BAKSI, A. K. 2014. The Deccan Trap – Cretaceous-Palaeogene boundary connection: new $^{40}Ar/^{39}Ar$ ages and critical assessment of existing argon data pertinent to this hypothesis. In: *Flood Basalts of Asia* (eds H. C. Sheth & L. Vanderkluysen), pp. 9–23. Journal of Asian Earth Sciences no. 84.

BEA, F., PEREIRA, M. D. & STROH, A. 1994. Mineral/leucosome trace element partitioning in a peraluminous migmatite (a laser ablation ICP-MS study). *Chemical Geology* **117**, 291–312.

BEARD, J.S. & LOFGREN, G.E. 1991. Dehydration melting and water-saturated melting of basaltic and andesitic greenstones and amphibolites at 1, 3 and 6.9 kb. *Journal of Petrology* **32**, 365–401.

BOWEN, N. L. 1928. *The Evolution of the Igneous Rocks*. Princeton University Press, Princeton, New Jersey, 334 p.

BOYNTON, W. B. 1984. Cosmochemistry of rare earth elements: meteorite studies. In: *Rare Earth Element Geochemistry* (ed P. Henderson), pp. 63–114. Elsevier, Amsterdam.

CHANDRASEKHAR, D. V., MISHRA, D. C., POORNACHANDRA RAO, G. V. S. & MALLIKHARJUNA RAO, J. 2002. Gravity and magnetic signatures of volcanic plugs related to Deccan volcanism in Saurashtra, India and their physical and geochemical properties. *Earth and Planetary Science Letters* **201**, 277–292.

CHATTERJEE, S. K. 1932. Igneous rocks from west Gir forest, Kathiawar. *The Journal of Geology* **40**, 155–160.

CHATTERJEE, A. C. 1961. Petrology of the lavas of Pavagad Hill, Gujarat. *Journal of Geological Society of India* **2**, 61–77.

CHATTERJEE, N. & BHATTACHARJI, S. 2001. Origin of the felsic and basaltic dykes and flows in the Rajula-Palitana-Sihor area of the Deccan Traps, Saurashtra, India: a geochemical and geochronological study. *International Geology Review* **43**, 1094–1116.

CHATTERJEE, N. & BHATTACHARJI, S. 2004. A preliminary geochemical study of zircons and monazites from Deccan felsic dykes, Rajula, Gujarat, India: implications for crustal melting. In: *Magmatism in India through Time* (eds H. C. Sheth & K. Pande), pp. 533–542. Proceedings of the Indian Academy of Sciences (Earth and Planetary Sciences) no. 113.

CLEVERLY, R.W., BETTON, P. J. & BRISTOW, J.W. 1984. Geochemistry and petrogenesis of the Lebombo rhyolites. In: *Petrogenesis of the Volcanic Rocks of the Karoo Province* (ed A. J. Erlank), pp. 171–194. Geological Society of South Africa Special Publication no. 13.

COBLE, M. A. & MAHOOD, G. A. 2012. Initial impingement of the Yellowstone plume located by widespread silicic volcanism contemporaneous with Columbia River flood basalts. *Geology* **40**, 655–658.

COLGAN, J. P., DUMITRU, T. A., MCWILLIAMS, M. & MILLER, E. L. 2006. Timing of Cenozoic volcanism and Basin and Range extension in northwestern Nevada: new constraints from the northern Pine Forest Range. *Geological Society of America Bulletin* **118**, 126–139.

COLÓN, D. P., BINDEMAN, I. P., ELLIS, B. S., SCHMITT, A. K. & FISHER, C. M. 2015. Hydrothermal alteration and melting of the crust during the Columbia River Basalt-Snake River Plain transition and the origin of low-$\delta^{18}O$ rhyolites of the central Snake River Plain. *Lithos* **224-225**, 310–323.

CUCCINIELLO, C., LANGONE, A., MELLUSO, L., MORRA, V., MAHONEY, J. J., MEISEL, T. & TIEPOLO, M. 2010. U-Pb ages, Pb-Os isotopes ratios, and platinum-group element (PGE) composition of the West-Central Madagascar flood basalt province. *Journal of Geology* **118**, 523–541.

CUCCINIELLO, C., CONRAD, J., GRIFA, C., MELLUSO, L., MERCURIO, M., MORRA, V., TUCKER, R. D. & VINCENT, M. 2011. Petrology and geochemistry of Cretaceous mafic and silicic dykes and spatially associated lavas in central-eastern coastal Madagascar. In: *Dyke Swarms: Keys for Geodynamic Interpretation* (ed R. K. Srivastava), pp. 345–375. Springer Verlag.

CUCCINIELLO, C., DEMONTEROVA, E. I., SHETH, H., PANDE, K. & VIJAYAN, A. 2015. $^{40}Ar/^{39}Ar$ geochronology and geochemistry of the Central Saurashtra mafic dyke swarm: insights into magmatic evolution, magma transport, and dyke-flow relationships in the northwestern Deccan Traps. *Bulletin of Volcanology* **77**, art. 45, doi: 10.1007/s00445-015-0932-0.

DAVE, S. S. 1971. The geology of the igneous complex of the Barda hills, Saurashtra, Gujarat state (India). *Bulletin of Volcanology* **35**, 619–632.

DE, A. 1981. Late Mesozoic – Lower Tertiary magma types of Kutch and Saurashtra. In: *Deccan Volcanism* (eds K. V. Subbarao, & R. N. Sukheswala), pp. 327–339. Geological Society of India Memoir no. 3.

DE, A. & BHATTACHARYYA, D. 1971. Phase-petrology with special reference to pyroxenes of the acid igneous complex of Barda Hills, western Saurashtra (Gujarat). *Bulletin of Volcanology* **35**, 907–929.

ELLIS, B. S., WOLFF, J. A., BOROUGHS, S., MARK, D. F., STARKEL, W. A. & BONNICHSEN, B. 2013. Rhyolitic volcanism of the central Snake River Plain: a review. *Bulletin of Volcanology* **75**, art. 745, doi: 10.1007/s00445-013-0745-y.

FEDDEN, F. 1884. *The Geology of the Kathiawar Peninsula in Gujarat*. Geological Survey of India Memoir 21, Pt. 2.

GARLAND, F. E., HAWKESWORTH, C. J. & MANTOVANI, M. S. M. 1995. Description and petrogenesis of the Paraná rhyolites. *Journal of Petrology* **36**, 1193–1227.

GOPALAN, K., TRIVEDI, J. R., MERH, S. S., PATEL, P. P. & PATEL, S. G. 1979. Rb–Sr age of Godhra and related granites, Gujarat, India. *Proceedings of the Indian Academy of Sciences (Earth and Planetary Sciences)* **4**, 7–17.

GOPALAN, K., MACDOUGALL, J. D., ROY, A. B. & MURALI, A. V. 1990. Sm-Nd evidence for 3.3 Ga old rocks in Rajasthan, northwestern India. *Precambrian Research* **48**, 287–297.

HELZ, R. T. 1976. Phase relations of basalts in their melting ranges at P_{H2O} = 5 kb. Part II: Melt compositions. *Journal of Petrology* **17**, 139–193.

HUANG, W. L. & WYLLIE, P. J. 1975. Melting reactions in the system $NaAlSi_3O_8$-$KAlSi_3O_8$-SiO_2, to 35 kilobars, dry and with excess water. *Journal of Geology* **83**, 737–748.

JAYANANDA, M., CHARDON, D., PEUCAT, J. J. & CAPDEVILA, R. 2006. 2.61 Ga potassic granites and crustal reworking in the western Dharwar craton, south India: tectonic, geochronologic and geochemical constraints. *Precambrian Research* **150**, 1–26.

KRISHNAMACHARLU, T. 1972. Petrology of picrodolerites from the Dedan cluster, Gujarat. *Journal of Geological Society of India* **13**, 262–272.

KRISHNAMURTHY, P. & COX, K. G. 1977. Picrite basalts and related lavas from the Deccan Traps of western India. *Contributions to Mineralogy and Petrology* **62**, 53–75.

KRISHNAMURTHY, P. & COX, K. G. 1980. A potassium-rich alkalic suite from the Deccan Traps, Rajpipla, India. *Contributions to Mineralogy and Petrology* **73**, 179–189.

KRISHNAN, M. S. 1926. *The petrography of rocks from the Girnar and Osham hills, Kathiawar*. Records of the Geological Survey of India 58, 380 p.

LE BAS, M. J., LE MAITRE, R. W., STRECKEISEN, A. & ZANETTIN, P. 1986. A chemical classification of volcanic rocks based on the total alkali-silica diagram. *Journal of Petrology* **27**, 745–750.

LEEMAN, W. P. & DASCH, E. J. 1978. Strontium, lead and oxygen isotopic investigation of the Skaergaard intrusion, east Greenland. *Earth and Planetary Science Letters* **41**, 47–51.

LELE, V. S. 1973. The Miliolite Limestone of Saurashtra, western India. *Sedimentary Geology* **10**, 301–310.

LEPAGE, L. D. 2003. ILMAT: an Excel worksheet for ilmenite–magnetite geothermometry and geobarometry. *Computers and Geosciences* **29**, 673–678.

LIGHTFOOT, P. C., HAWKESWORTH, C. J. & SETHNA, S. F. 1987. Petrogenesis of rhyolites and trachytes from the Deccan Trap: Sr, Nd, and Pb isotope and trace element evidence. *Contributions to Mineralogy and Petrology* **95**, 44–54.

LUDWIG, K. R. 2012. *Isoplot/Ex, v. 3.75*. Berkeley Geochronology Center Special Publication No. 5, Berkeley.

LUTH, W. C., JAHNS, R. H. & TUTTLE, O. F. 1964. The granite system at pressures of 4 to 10 kilobars. *Journal of Geophysical Research* **69**, 759–773.

LYUBETSKAYA, T. & KORENAGA, J. 2007. Chemical composition of Earth's primitive mantle and its variance: 1. Method and results. *Journal of Geophysical Research* **112**, B03211, doi:10.1029/2005JB004223.

MAHONEY, J. J., MACDOUGALL, J. D., LUGMAIR, G. W., GOPALAN, K. & KRISHNAMURTHY, P. 1985. Origin of contemporaneous tholeiitic and K-rich alkalic lavas: a case study

from the northern Deccan Plateau, India. *Earth and Planetary Science Letters* **72**, 39–53.

MAHONEY, J. J., SAUNDERS, A. D., STOREY, M. & RANDRIAMANANTENASOA, A. 2008. Geochemistry of the Volcan de l'Androy basalt-rhyolite complex, Madagascar Cretaceous igneous province. *Journal of Petrology* **49**, 1069–1096.

MAITHANI, P. B., GOYAL, N., BANERJEE, R., GURJAR, R., RAMCHANDRAN, S. & SINGH, R. 1996. Rhyolites of Osham hills, Saurashtra, India: a geochemical study. *Gondwana Geological Magazine Special Volume* **2**, 213–224.

MARATHE, A. R., RAJAGURU, S. N. & LELE, V. S. 1977. On the problem of the origin and age of the Miliolite rocks of the Hiran valley, Saurashtra, India. *Sedimentary Geology* **19**, 197–215.

MATHUR, K. K., DUBEY, V. S. & SHARMA, N. L. 1926. Magmatic differentiation in Mount Girnar. *The Journal of Geology* **34**, 289–307.

MCCURRY, M., HAYDEN, K. P., MORSE, L. H. & MERTZMAN, S. 2008. Genesis of post-hotspot, A-type rhyolite of the Eastern Snake River Plain volcanic field by extreme fractional crystallization of olivine tholeiite. *Bulletin of Volcanology* **70**, 361–383.

MELLUSO, L., BECCALUVA, L., BROTZU, P., GREGNANIN, A., GUPTA, A. K., MORBIDELLI, L. & TRAVERSA, G. 1995. Constraints on the mantle sources of the Deccan Traps from the petrology and geochemistry of the basalts of Gujarat State (western India). *Jornal of Petrology* **36**, 1393–1432.

MELLUSO, L., MORRA, V., BROTZU, P. & MAHONEY, J. J. 2001. The Cretaceous igneous province of Madagascar: geochemistry and petrogenesis of lavas and dikes from the central–western sector. *Journal of Petrology* **42**, 1249–1278.

MELLUSO, L., CUCCINIELLO, C., PETRONE, C. M., LUSTRINO, M., MORRA, V., TIEPOLO, M. & VASCONCELOS, L. 2008. Petrology of Karoo volcanic rocks in the southern

Lebombo monocline, Mozambique. *Journal of African Earth Sciences* **52**, 139–151.

MISRA, K. S. 1981. The tectonic setting of Deccan volcanics in southern Saurashtra and northern Gujarat. In: *Deccan Volcanism* (eds K. V. Subbarao & R. N. Sukheswala), pp.81–86. Geological Society of India Memoir no. 3.

MOORBATH, S. & BELL, J. D. 1965. Strontium isotope abundance studies and rubidium-strontium age determinations on Tertiary igneous rocks from the Isle of Skye, north-west Scotland. *Journal of Petrology* **6**, 37–66.

NEDELEC, A., STEPHENS, W. E. & FALLICK, A. E. 1995. The Panafrican stratoid granites of Madagascar: alkaline magmatism in a post-collisional extensional setting. *Journal of Petrology* **36**, 1367–1391.

PARISIO, L., JOURDAN, F., MARZOLI, A., MELLUSO, L., SETHNA, S. F. & BELLIENI, G. 2016. $^{40}Ar/^{39}Ar$ ages of alkaline and tholeiitic rocks from the northern Deccan Traps: implications for magmatic processes and the K-Pg boundary. *Journal of the Geological Society of London* **173**, 679–688.

PAUL, D. K., POTTS, P. J., REX, D. C. & BECKINSALE, R. D. 1977. Geochemical and petrogenetic study of the Girnar igneous complex, Deccan volcanic province, India. *Geological Society of America Bulletin* **88**, 227–234.

PENG, Z. X., MAHONEY, J. J., HOOPER, P., HARRIS, C. & BEANE, J. 1994. A role for lower continental crust in flood basalt genesis? Isotopic and incompatible element study of the lower six formations of the western Deccan Traps. *Geochimica et Cosmochimica Acta* **58**, 267–288.

POUCHOU, J. L. & PICHOIR, F. 1988. A simplified version of the "PAP" model for matrix corrections in EPMA. In: *Microbeam Analysis* (ed D. E. Newbury), pp. 315–318. San Francisco Press, San Francisco.

PUTIRKA K. 2008. Thermometers and barometers for volcanic systems. In: *Minerals, Inclusions and Volcanic Processes* (eds K. Putirka & F. Tepley), pp. 61–120. Reviews in Mineralogy and Geochemistry 69, American Mineralogical Society, Washington, D.C.

RENNE, P. R., SWISHER, C. C., DEINO, A. L., KARNER, D. B., OWENS, T. L. & DEPAOLO, D. J. 1998. Intercalibration of standards, absolute ages and uncertainties in $^{40}Ar/^{39}Ar$ dating. *Chemical Geology* **145**, 117–152.

RILEY, T. R., LEAT, P. T., PANKHURST, R. J. & HARRIS, C. 2001. Origins of large-volume rhyolitic volcanism in the Antarctic Peninsula and Patagonia by crustal melting. *Journal of Petrology* **42**, 1043–1065.

SCHAIRER, J. F. & BOWEN, N. L. 1935. Preliminary report on equilibrium relations between feldspathoids, alkali feldspars, and silica. *Transactions of the American Geophysical Union* **16**, 325–328.

SCHNETGER, B. 1994. Partial melting during the evolution of the amphibolite- to granulite-facies gneisses of the Ivrea Zone, northern Italy. *Chemical Geology* **113**, 71–101.

SCHOENE, B., SAMPERTON, K. M., EDDY, M. P., KELLER, G., ADATTE, T., BOWRING, S., KHADRI, S. F. R. & GERTSCH, B. 2015. U-Pb geochronology of the Deccan Traps and relation to the end-Cretaceous mass extinction. *Science* **347**, 182-184.

SEN, G. 1980. Mineralogical variations in the Delakhari Sill, Deccan Trap intrusion, central India. *Contributions to Mineralogy and Petrology* **75**, 71–78.

SEN, A., PANDE, H., HEGNER, E., SHARMA, K. K., DAYAL, A. M., SHETH, H. C. & MISTRY, H. 2012. Deccan volcanism in Rajasthan: ^{40}Ar-^{39}Ar geochronology and geochemistry of the Tavidar volcanic suite. *Journal of Asian Earth Sciences* **59**, 127–140.

SHELLNUTT, J. G., BHAT, G. M., WANG, K.-L., BROOKFIELD, M. E., DOSTAL, J. & JAHN, B.-M. 2012. Origin of the silicic volcanic rocks of the Early Permian Panjal Traps, Kashmir, India. *Chemical Geology* **334**, 154–170.

SHETH, H. C. & MELLUSO, L. 2008. The Mount Pavagadh volcanic suite, Deccan Traps: geochemical stratigraphy and magmatic evolution. *Journal of Asian Earth Sciences* **32**, 5–21.

SHETH, H. C. & PANDE, K. 2014. Geological and $^{40}Ar/^{39}Ar$ age constraints on late-stage Deccan rhyolitic volcanism, inter-volcanic sedimentation, and the Panvel flexure from the Dongri area, Mumbai. In: *Flood Basalts of Asia* (eds H. C Sheth & L. Vanderkluysen), pp. 167–175. Journal of Asian Earth Sciences no. 84.

SHETH, H. C., CHOUDHARY, A. K., BHATTACHARYYA, S., CUCCINIELLO, C., LAISHRAM, R. & GURAV, T. 2011. The Chogat-Chamardi subvolcanic complex, Saurashtra, northwestern Deccan Traps: geology, petrochemistry, and petrogenetic evolution. *Journal of Asian Earth Sciences* **41**, 307–324.

SHETH, H. C., CHOUDHARY, A. K., CUCCINIELLO, C., BHATTACHARYYA, S., LAISHRAM, R. & GURAV, T. 2012. Geology, petrochemistry, and genesis of the bimodal lavas of Osham Hill, Saurashtra, northwestern Deccan Traps. *Journal of Asian Earth Sciences* **43**, 176–192.

SOESOO, A. 2000. Fractional crystallization of mantle-derived melts as a mechanism for some I-type granite petrogenesis: an example from Lachlan fold belt, Australia. *Journal of Geological Society London* **157**, 135–149.

SPULBER, S. D. & RUTHERFORD, M. J. 1983. The origin of rhyolite and plagiogranite in oceanic crust: an experimental study. *Journal of Petrology* **24**, 1–25.

SUBBA RAO, S. 1971. Petrogenesis of acid rocks of the Deccan Traps. *Bulletin of Volcanology* **35**, 983–997.

STEINER, J.C., JAHNS, R. H. & LUTH, W. C. 1975. Crystallization of alkali feldspar and quartz in the haplogranite system $NaAlSi_3O_8$-$KAlSi_3O_8$-SiO_2-H_2O at 4 kb. *Geological Society of America Bulletin* **86**, 83–98.

TURNER, S. P., FODEN, J. D. & MORRISON, R. S. 1992. Derivation of some A-type magmas by fractionation of basaltic magma: an example from the Padthaway Ridge, South Australia. *Lithos* **28**, 151–179.

TUTTLE, O. F. & BOWEN, N. L. 1958. *Origin of granite, in the light of experimental studies in the system $NaAlSi_3O_8$-$KAlSi_3O_8$-SiO_2-H_2O.* Geological Society of America Memoir 74, 153 p.

VANDERKLUYSEN, L., MAHONEY, J. J., HOOPER, P. R., SHETH, H. C. & RAY, R. 2011. The feeder system of the Deccan Traps (India): insights from dyke geochemistry. *Journal of Petrology* **52**, 315–343.

VAN DER LAAN, S. R. & WYLLIE, P. J. 1991. Constraints on Archaean trondhjemite genesis from hydrous crystallization experiments on Nuk gneiss at 10-17 kbar. *Journal of Geology* **100**, 57–68.

VERMA, S. P. 1999. Geochemistry of evolved magmas and their relationship to subduction-unrelated mafic volcanism at the volcanic front of the central Mexican Volcanic Belt. *Journal of Volcanology and Geothermal Research* **93**, 151–171.

VERMA, S. P., TORRES-ALVARADO, I. S. & SOTELO-RODRIGUEZ, Z. T. 2002. SINCLAS: Standard igneous norm and volcanic rock classification system. *Computers and Geosciences* **28**, 711–715.

WAKHALOO, S. N. 1967. *On the nature of volcanic eruption and of differentiation of the Girnar igneous complex, Junagarh, Kathiawar peninsula, India*. Proceedings of Symposium on Upper Mantle Project: Hyderabad: 430–449.

WEST, W. D. 1958. The petrography and petrogenesis of fortyeight flows of Deccan Trap penetrated by borings in western India. *Transactions of the National Institute of Sciences (India)* **4**, 1–56.

WHALEN, J. B., CURRIE, K. L. & CHAPPELL, B. W. 1987. A-type granites: geochemical characteristics, discrimination and petrogenesis. *Contributions to Mineralogy and Petrology* **95**, 407–419.

WHITAKER, M. L., NEKVASIL, H., LINDSLEY, D. H. & MCCURRY, M. 2008. Can crystallization of olivine tholeiite give rise to potassic rhyolites? – an experimental investigation. *Bulletin of Volcanology* **70**, 417–434.

WICKHAM, S. M., ALBERTS, A. D., LITVINOVSKY, B. A., BINDEMAN, I. N. & SCHAUBLE, E. A. 1996. A stable isotope study of anorogenic magmatism in East Central Asia. *Journal of Petrology* **37**, 1063–1095.

WINTHER, K. C. & NEWTON, R. C. 1991. Experimental melting of hydrous low-K tholeiite: evidence on the origin of Archaean cratons. *Bulletin of the Geological Society of Denmark* **39**, 213–228.

WOLF, M. B. & WYLLIE, P. J. 1994. Dehydration-melting of amphibolite at 10 kbar; the effects of temperature and time. *Contributions to Mineralogy and Petrology* **115**, 369–383.

ZELLMER, G. F., RUBIN, K. H., GRÖNVOLD, K. & JURADO-CHICHAY, Z. 2008. On the recent bimodal magmatic processes and their rates in the Torfajökull-Veidivötn area, Iceland. *Earth and Planetary Science Letters* **269**, 388–398.

ZHU, B., PEATE, D. W., GUO, Z. & LIU, R. 2017. Crustally derived granites in Dali, SW China: new constraints on silicic magmatism of the Central Emeishan large igneous province. *International Journal of Earth Sciences* **106**, 2503–2525.

Table captions

Table 1. Representative chemical analyses (in wt.%) of feldspars in the Barda-Alech rocks, Saurashtra, northwestern Deccan Traps

Table 2. Representative chemical analyses (in wt.%) of pyroxenes in the Barda rocks, Saurashtra

Table 3. Representative chemical analyses (in wt.%) of magnetites and ilmenites in the Barda rocks, Saurashtra

Table 4. Representative chemical analyses (in wt.%) of zircons, titanites, apatites and monazites in the Barda-Alech rocks, Saurashtra

Table 5. Summary of $^{40}Ar/^{39}Ar$ dating results for granophyres of the Barda complex, Saurashtra

Table 6. Major and trace element data for rocks of the Barda and Alech complexes, Saurashtra

Table 7. Sr and Nd isotopic data for rocks of the Barda and Alech complexes, Saurashtra

Supplementary Table S1. Argon isotopic composition (corrected for blank, mass discrimination and interference), Apparent Age and percentage of nucleogenic and

radiogenic argon for samples BR3, BR5 and BR7 WR. Errors on age are without and (with) error on J respectively. Errors quoted are 2σ

Supplementary Table S2. CIPW norms of the Barda and Alech rocks

Figure captions

Fig. 1. Simplified geological maps of the Deccan Traps (a) and of Saurashtra (b), with the important central complexes and locations in Saurashtra marked (after De, 1981; Misra, 1981).

Fig. 2. Topography and localities in the Barda and Alech complexes, Saurashtra, with the sample locations marked. Numbers within grey ellipses are the numbers of the Survey of India topographic sheets of 1:50,000 scale, and numbers near triangles are the elevations of points above mean sea level.

Fig. 3. Field photographs showing (a) imposing landscape of the granophyre hills near Porbandar, Barda complex. Building and farmers provide a scale. (b) Flow folding in brown Alech rhyolite (sample AL7) near Dhoriyo Nes. Person provides a scale.

Fig. 4. Photomicrographs and backscattered electron (BSE) images of the Barda and Alech rocks. (a) Granophyre BR5 with typical granophyric intergrowths of quartz and alkali feldspar (crossed nicols). (b) Granophyre BR11 with alkali feldspar, quartz, plagioclase, clinopyroxene and magnetite (BSE). (c) Basaltic andesite dyke BR4 with crustal basement xenoliths (crossed nicols). (d) Groundmass of dyke BR4 with clinopyroxene, plagioclase,

orthopyroxene, quartz, magnetite and ilmenite (BSE). (e) Granoblastic-polygonal texture (with quartz, orthopyroxene, plagioclase, alkali feldspar and magnetite) in quartzite basement xenolith in dyke BR4 (BSE). (f) Rhyolite AL4 with alkali feldspar microphenocryst in a groundmass of alkali feldspar and quartz (BSE). Mineral names have been abbreviated as follows: afs, alkali feldspar; cpx, clinopyroxene; opx, orthopyroxene; qz, quartz; mgt, magnetite; ilm, ilmenite; plag, plagioclase.

Fig. 5. Mineral compositions. (a) Feldspar compositions observed in the Barda and Alech rocks. (b) Pyroxene compositions of Barda-Alech rocks projected in the Ca-Mg-Fe quadrilateral. Grey shaded field contains pyroxene analyses for all analyzed Deccan rocks taken together (Cucciniello *et al*. 2015 and references therein).

Fig. 6. $^{40}Ar/^{39}Ar$ plateau spectra (left panels) and isochron plots (right panels) for the Barda granophyre samples (a) BR3, (b) BR5, and (c) BR12. In the plateau spectra, the plateau steps are shown with red outlines and the non-plateau steps with dark blue outlines. Also shown are values of the MSWD (mean square weighted deviate) and probability (*p*). Inset figures show the enlarged views of the plateau spectra.

Fig. 7. (a) Chondrite-normalized REE patterns of the Barda rocks. Chondrite normalizing values are from Boynton (1984). Also shown for comparison are patterns of some silicic rocks of the Chogat-Chamardi complex (Sheth *et al*. 2011). (b) Primitive mantle-normalized multielement patterns of the Barda rocks. Normalizing values are from Lyubetskaya & Korenaga (2007).

Fig. 8. (a) Chondrite-normalized REE patterns of the Alech rocks. Chondrite normalizing values are from Boynton (1984). Also shown for comparison are patterns of Osham Hill rhyolitic rocks (Sheth *et al*. 2012). (b) Primitive mantle-normalized multielement patterns of the Alech rocks. Normalizing values are from Lyubetskaya & Korenaga (2007). (c) Comparison of the primitive mantle-normalized multielement patterns of Check Hill rhyolite AL10 and dacite dyke AL11, Alech complex.

Fig. 9. Sr-Nd isotopic plot showing data for Deccan Traps silicic rocks, including the Barda-Alech silicic rocks (this study). Data sources are: Rajpipla rhyolite (Mahoney *et al*. 1985), Mumbai rhyolites (Lightfoot, Hawkesworth & Sethna, 1987), Chamardi granophyres and microgranites and Chogat rhyolites (Sheth *et al*. 2011), Osham rhyolite and pitchstones (Sheth *et al*. 2012), and Tavidar rhyolites (Sen *et al*. 2012). Nd isotopic data are not available for the Pavagadh rhyolites (Sheth & Melluso, 2008), Mount Girnar silicic porphyry (Paul *et al*. 1977), and several other Mumbai rhyolites (Lightfoot, Hawkesworth & Sethna, 1987), whose Sr isotopic ranges are shown by grey bands under the main figure. Also shown in the background are Sr-Nd isotopic compositions of the Western Ghats stratigraphic formations (Peng *et al*. 1994; Vanderkluysen *et al*. 2011). All Sr-Nd isotopic data are initial ratios recalculated at 65 Ma and plotted for direct comparison. Note the large gap in Sr isotopic composition between the various silicic rocks. An enlarged view of the little-contaminated silicic rocks of the Deccan Traps, including the Barda-Alech samples of this study, is also provided as an inset figure.

Fig.10. Comparison of Barda-Alech silicic rock compositions with those of experimental liquids produced by partial melting of hydrated basaltic rocks, greenstones, and

amphibolites. Fields enclose the experimental data of Wolf & Wyllie (1994), Beard & Lofgren (1991), Spulberg & Rutherford (1983) and Helz (1976),

Fig. 11. Variation of Zr vs. Y, and La vs. Yb, for Barda-Alech silicic rocks compared with model results for batch partial melting of Deccan mafic rocks and closed-system fractional crystallization (FC) of Deccan mafic magmas. The values on the batch melting model are 5% melting increments for 5-20% melting. Fractional melting model results are similar to those of batch melting model. The total percentage of fractional crystallization is 90-95%; the model fractionation assemblage consists of plagioclase (49%), clinopyroxene (39%), titanomagnetite (11%), ± apatite (1%). The values along the FC curves indicate the residual liquid fraction. Data sources are Sheth *et al*. (2012, basaltic andesite OSH5), Melluso *et al*. (1995, low-Ti and high-Ti basalts) and this study (basaltic andesite BR4). The model source for batch melting has 40% plagioclase, 40% clinopyroxene, 10% olivine and 10% magnetite in the mode; melting of these minerals is assumed to occur in proportions of 75:15:5:5, respectively (Mahoney *et al*. 2008). The partition coefficients are from Mahoney *et al*. (2008) and EarthRef (https://earthref.org/KDD/).

Fig. 12. Qtz-Ab-Or system with the compositions of the Barda-Alech silicic rocks plotted. The Qtz-Ab-Or proportions have been calculated from the rocks' CIPW norms. The white circles correspond to water-saturated minima and eutectic compositions at 1 atmosphere and 0.5 to 10 kbar (Schairer & Bowen, 1935; Tuttle & Bowen 1958; Steiner, Jahns & Luth, 1975; Luth, Jahns & Tuttle, 1964). White triangles correspond to minima for the anhydrous system at 4 and 10 kbar (Steiner, Jahns & Luth, 1975; Huang & Wyllie, 1975).

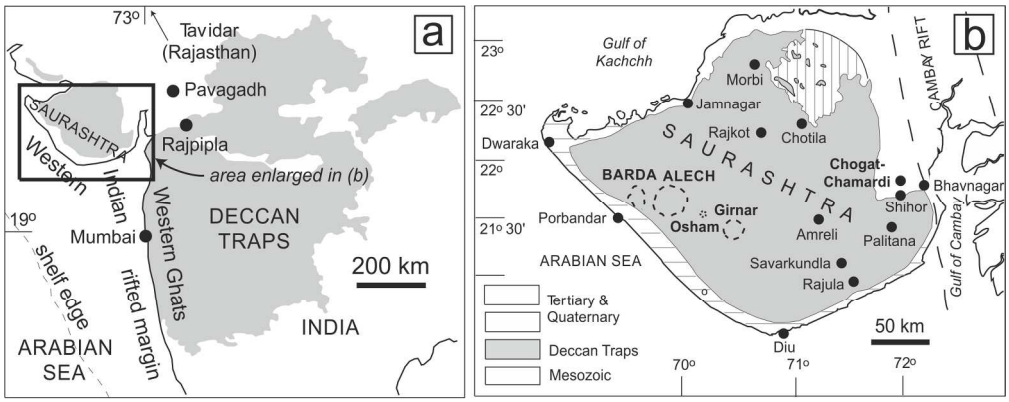

Figure 1

194x76mm (300 x 300 DPI)

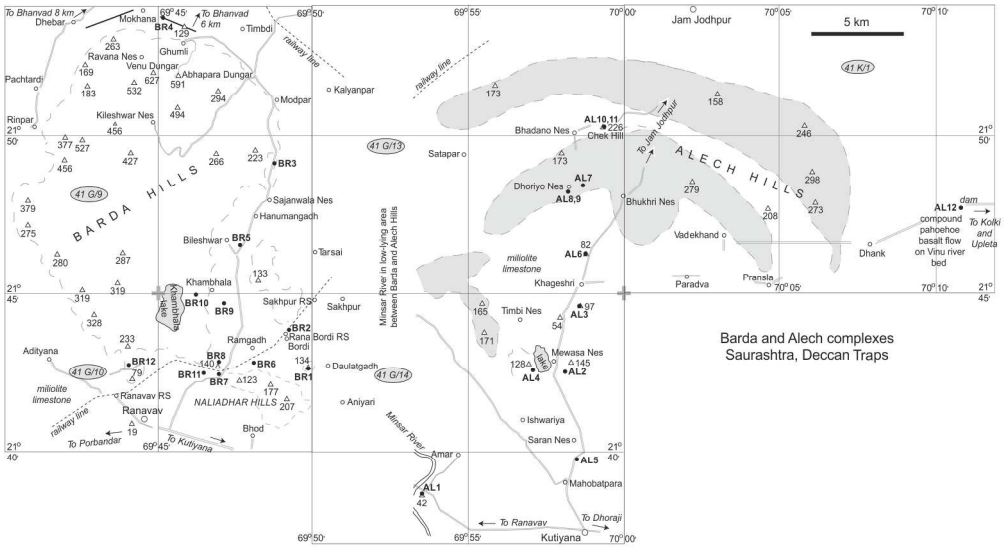

Figure 2

209x113mm (300 x 300 DPI)

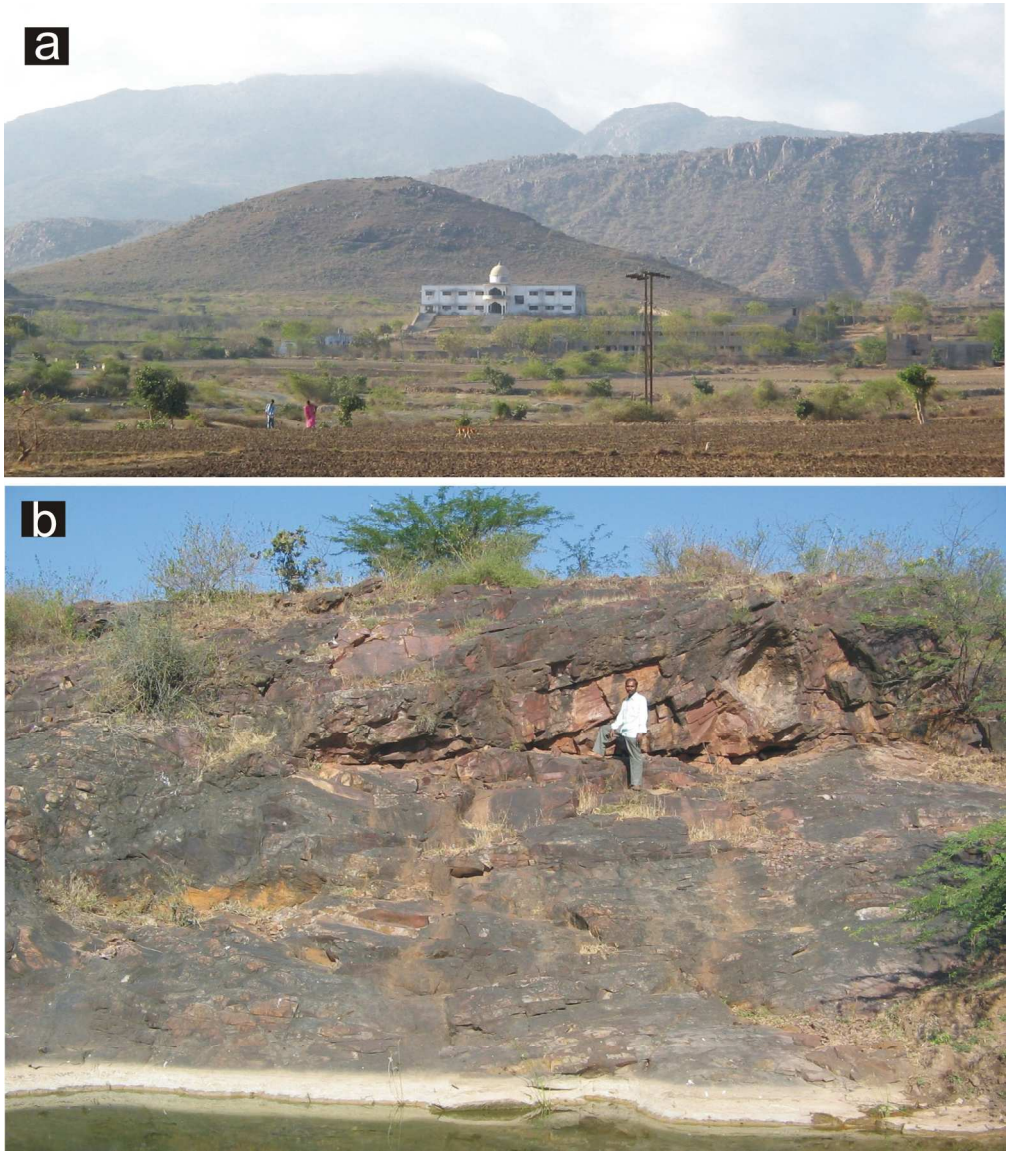

Figure 3

169x194mm (300 x 300 DPI)

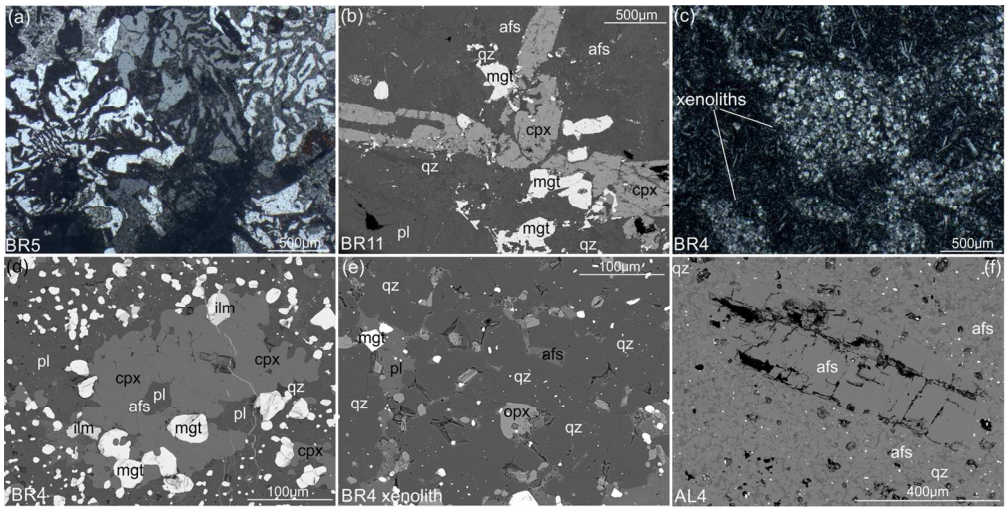

Figure 4

135x67mm (300 x 300 DPI)

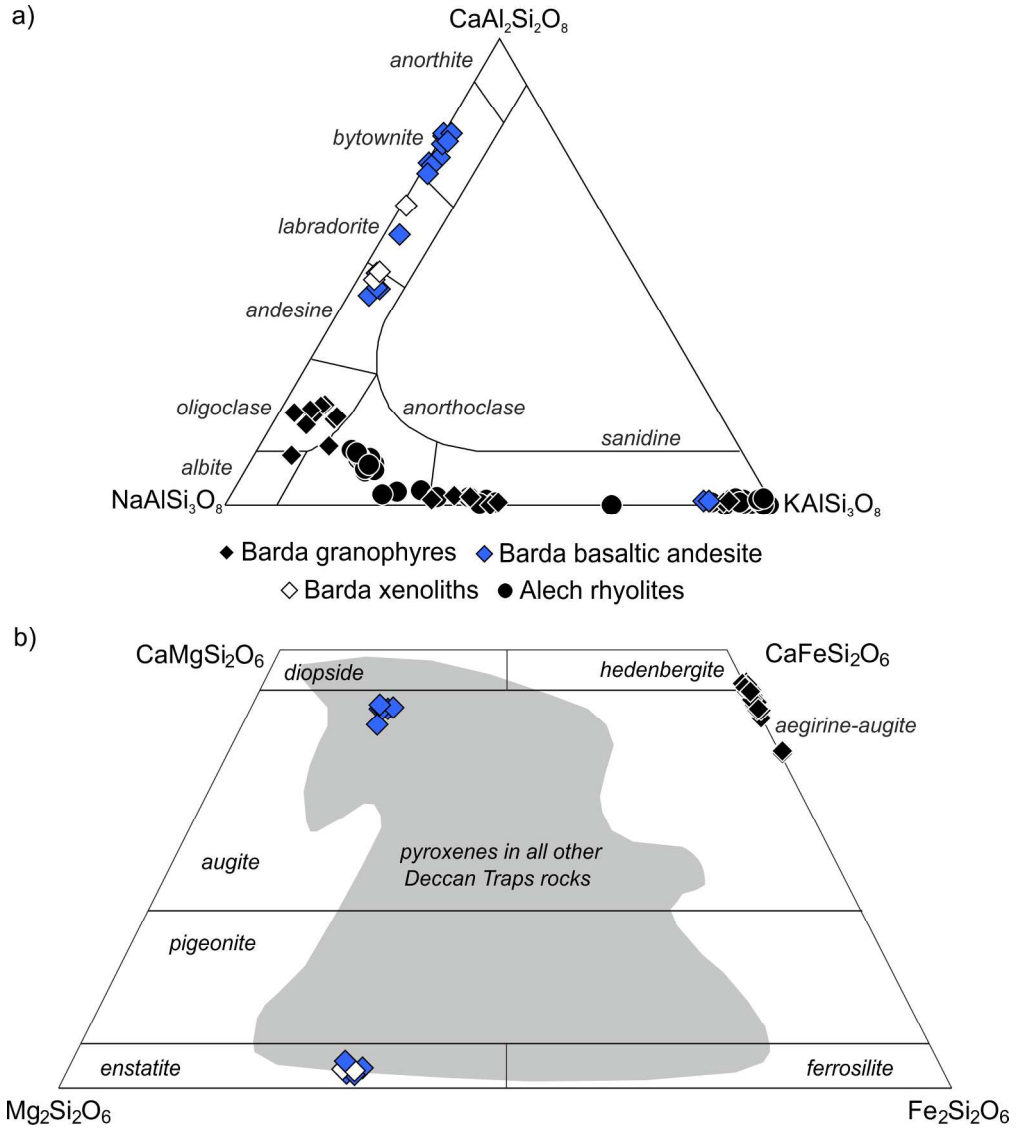

Figure 5

198x221mm (300 x 300 DPI)

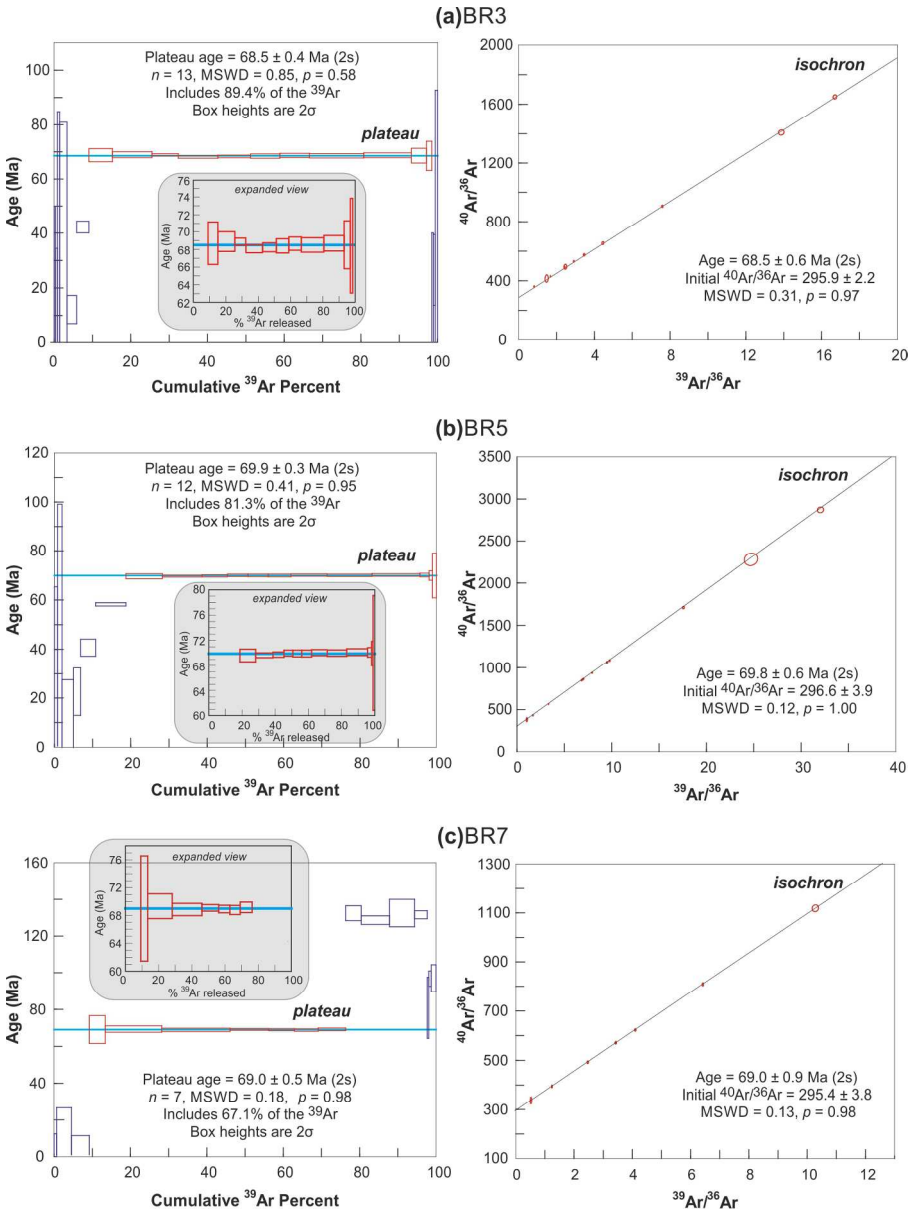

Figure 6

173x231mm (300 x 300 DPI)

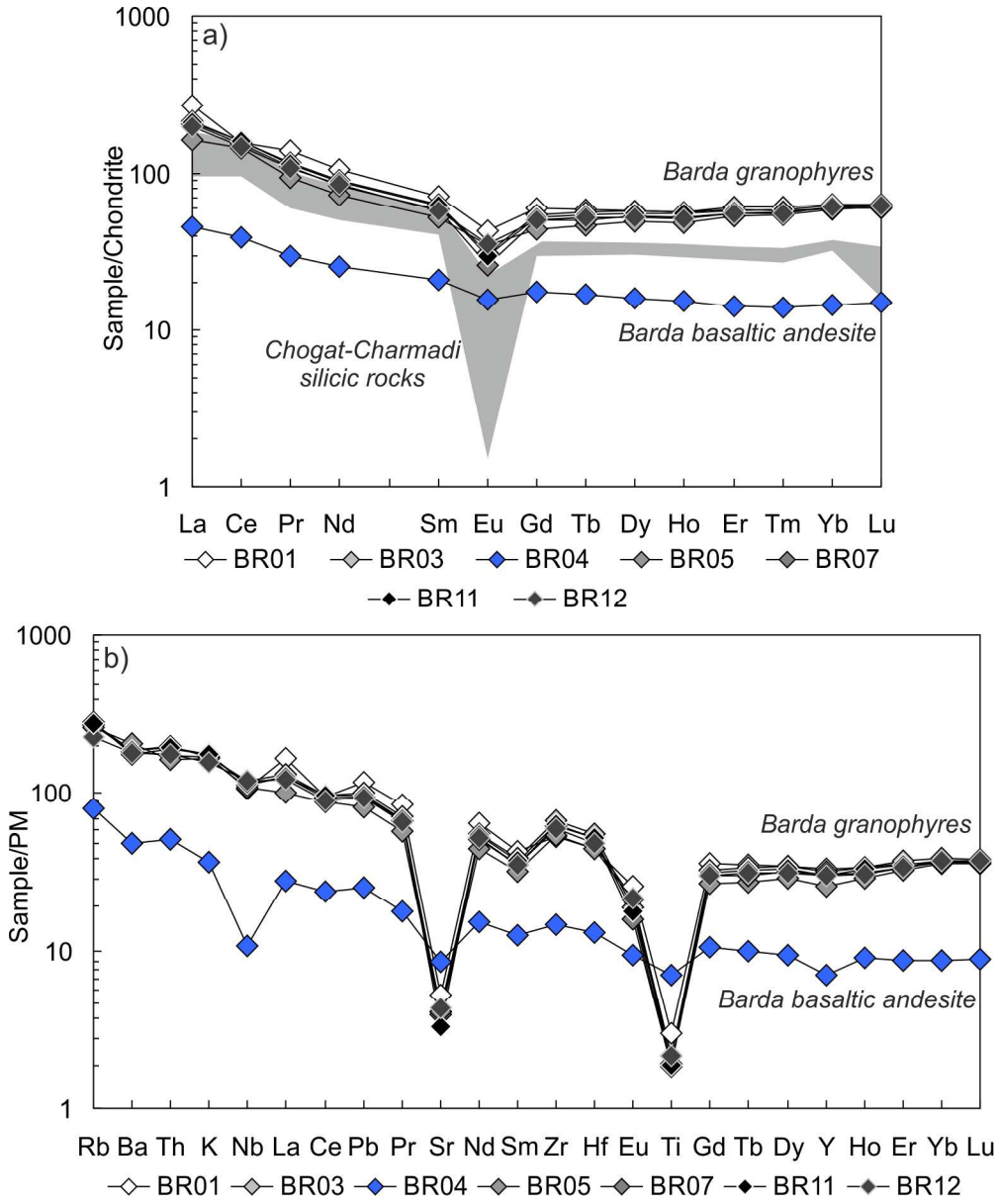

Figure 7

196x236mm (300 x 300 DPI)

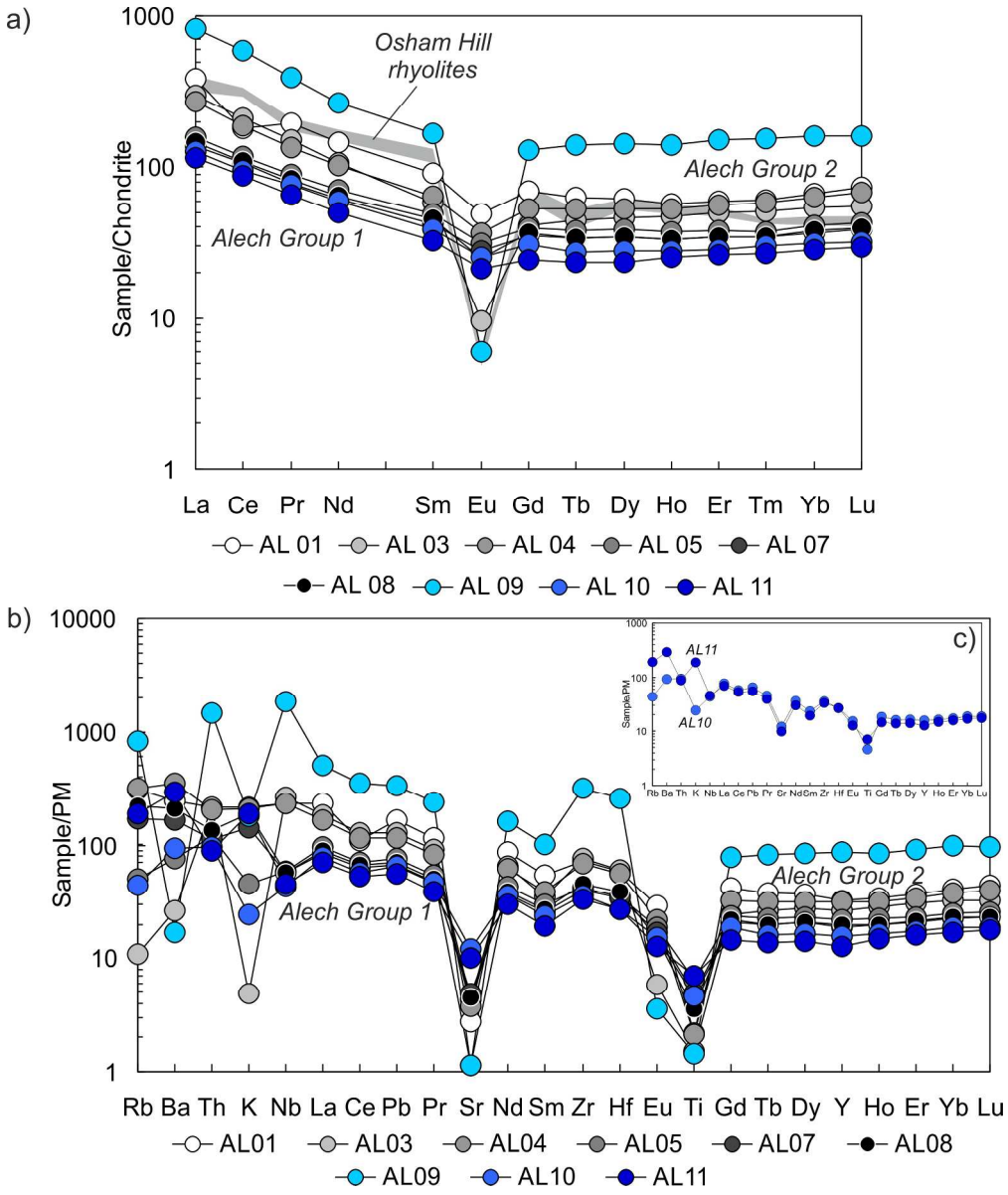

Figure 8

206x244mm (300 x 300 DPI)

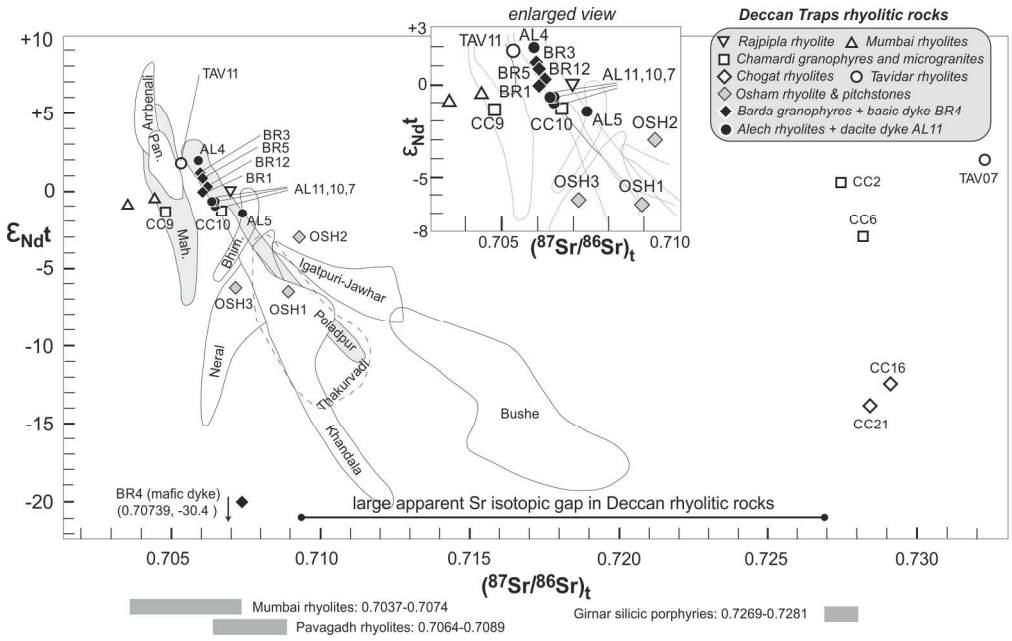

Figure 9

184x115mm (300 x 300 DPI)

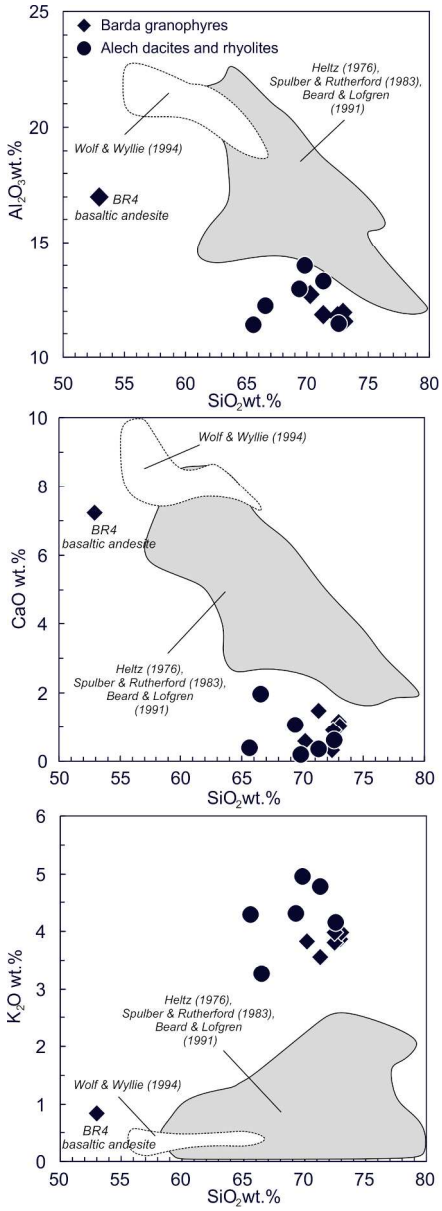

Figure 10

102x283mm (300 x 300 DPI)

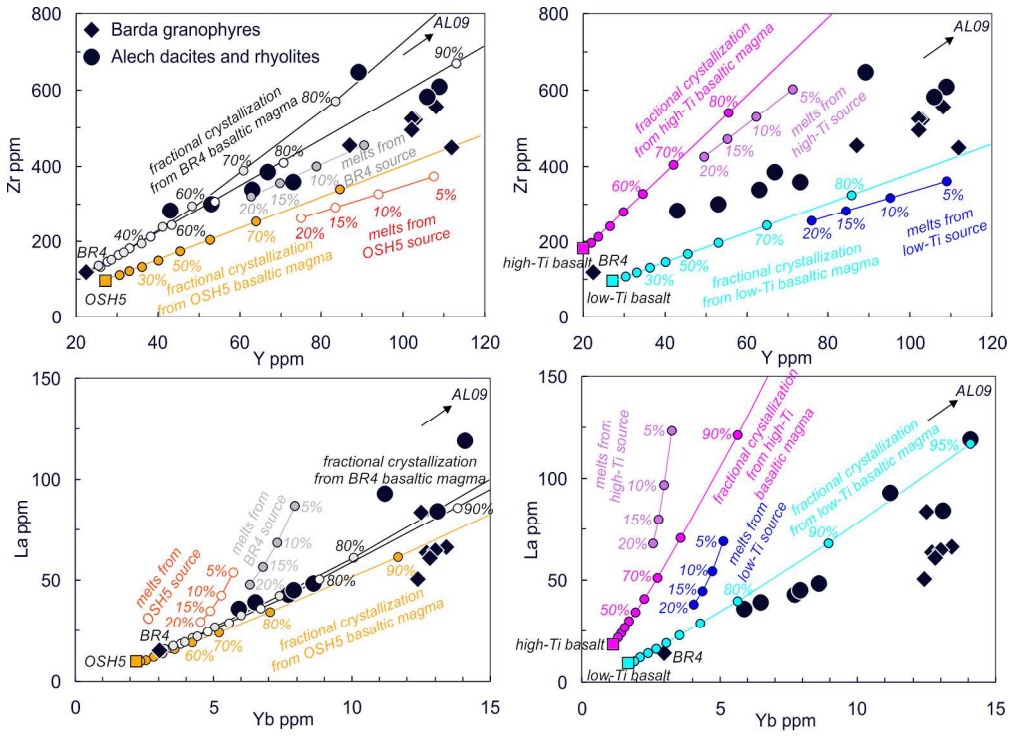

Figure 11

201x145mm (300 x 300 DPI)

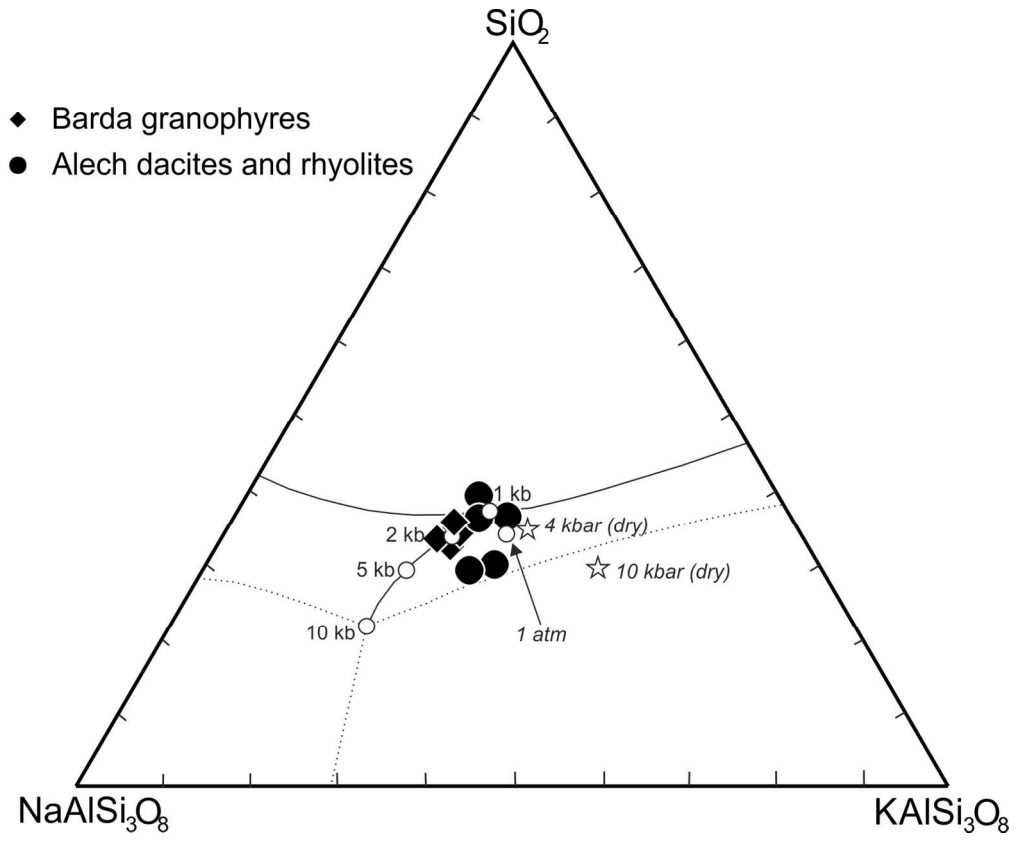

Figure 12

139x114mm (300 x 300 DPI)

Table 1: Representative chemical analyses (in wt.%) of feldspars in the Barda-Alech rocks, Saurashtra, northwestern Deccan Traps

Sample	Rock name	Mineral name	Description	SiO_2	Al_2O_3	FeO	CaO	Na_2O	K_2O	BaO	SrO	Sum	An	Ab	Or
BR3	gph	alk-feld	gm	66.39	18.58	0.68	0.23	7.05	6.57	0.22	0.60	100.32	1	62	37
BR3	gph	alk-feld	gm	63.58	18.45	0.32	0.21	0.70	15.75	0.11	0.64	99.75	1	8	91
BR3	gph	pl	core	62.02	22.65	0.34	4.54	8.37	1.21	0.43	0.00	99.55	21	71	7
BR3	gph	pl	rim	65.13	21.21	0.48	2.33	9.81	1.16	0.27	0.36	100.75	11	82	7
BR3	gph	pl	core	62.62	22.27	0.33	4.10	8.67	1.07	0.37	0.62	100.06	19	74	7
BR7	gph	alk-feld	core	65.28	18.07	0.73	0.10	1.17	15.27	0.12	0.32	101.07	0	11	88
BR7	gph	alk feld	gm	64.40	18.16	0.09	0.15	0.80	15.92	0.09	0.28	99.90	1	8	92
BR11	gph	pl	core	64.23	21.70	-	3.69	7.69	1.81	-	0.68	99.80	18	71	11
BR11	gph	pl	rim	64.16	22.03	0.19	3.55	7.24	1.73	0.05	0.27	99.22	19	70	11
BR11	gph	alk feld	core	67.42	18.40	0.46	0.37	5.93	6.73	0.10	0.90	100.31	2	57	41
BR11	gph	alk feld	rim	67.36	18.60	0.36	0.34	5.72	7.25	-	0.65	100.27	2	54	44
BR12	gph	pl	core	61.87	22.10	0.47	4.49	8.78	1.00	-	1.04	99.75	20	74	5
BR12	gph	pl	core	63.73	22.37	0.45	4.11	8.84	0.51	-	0.43	100.44	20	77	3
BR12	gph	pl	core	64.02	21.81	0.31	3.69	9.09	1.08	0.20	0.21	100.40	17	77	6
BR4	b.a.	pl	gm	56.65	25.80	0.88	9.12	5.67	0.53	0.42	0.29	99.35	45	51	4
BR4	b.a.	alk feld	gm	63.74	18.56	0.80	0.17	1.31	14.95	0.69	0.34	100.55	1	12	87
BR4	b.a.	pl	core	47.82	32.17	0.49	16.38	2.26	-	-	0.21	99.33	80	20	0
BR4	b.a.	pl	rim	47.06	33.21	0.67	16.29	2.14	0.11	0.49	-	99.97	80	19	2
BR4	b.a.	pl	core	47.34	31.36	1.16	15.66	2.18	0.22	0.13	0.34	98.38	78	21	2
BR4	b.a.	pl	rim	56.69	26.70	0.83	9.23	5.33	0.69	0.53	0.00	100.00	46	49	5
BR4	b.a.	pl	gm	55.14	27.87	0.85	10.62	5.47	0.50	-	0.36	100.81	50	47	3
BR4	xen	pl	core	51.64	29.20	0.41	13.26	3.87	0.16	-	0.38	98.91	64	35	1
BR4	xen	pl	core	56.04	27.25	1.09	9.98	5.54	0.50	0.13	-	100.53	48	49	3
AL2	rhy	alk feld	core	66.39	21.01	0.44	1.78	7.62	3.67	0.58	-	101.49	9	68	23
AL2	rhy	alk feld	rim	65.97	20.86	-	2.16	7.83	3.71	0.10	0.12	100.75	10	68	21
AL2	rhy	alk feld	gm	66.45	19.81	0.27	0.63	6.71	5.51	0.17	0.09	99.65	3	63	34
AL2	rhy	alk feld	gm	66.26	18.24	0.76	0.24	5.53	7.77	0.08	0.38	99.26	1	52	47
AL2	rhy	alk feld	mcr	65.71	19.09	0.41	0.31	5.71	6.96	0.98	0.80	99.97	2	55	44
AL4	rhy	alk feld	core	66.05	20.51	0.00	1.49	7.64	3.90	0.44	0.56	100.59	7	69	24
AL4	rhy	alk feld	rim	65.78	20.68	0.28	2.11	7.71	3.19	0.32	0.62	100.69	10	70	19
AL4	rhy	alk feld	core	65.44	20.30	0.68	1.51	7.70	3.46	0.51	-	99.60	8	71	22
AL4	rhy	alk feld	rim	64.64	20.98	0.64	2.28	7.72	3.07	0.20	0.47	99.99	11	70	18
AL4	rhy	alk feld	gm	65.80	20.91	0.38	1.63	7.40	3.49	0.28	0.13	100.03	8	70	22
AL4	rhy	alk feld	gm	66.75	19.46	0.45	0.48	7.82	4.58	0.61	0.56	100.70	2	70	28
AL9	rhy	alk feld	gm	63.88	17.86	0.07	0.08	0.55	16.69	-	0.16	99.29	0	5	94
AL9	rhy	alk feld	gm	64.16	17.96	0.45	0.25	0.55	16.49	-	-	99.86	1	5	94
AL9	rhy	alk feld	gm	64.39	18.52	0.17	0.29	0.61	15.62	0.08	0.27	99.96	1	6	92
AL8	rhy	alk feld	gm	66.99	19.01	0.45	-	2.87	10.83	0.27	0.43	100.85	0	29	71
AL8	rhy	alk feld	gm	64.23	18.91	1.17	0.09	0.18	16.09	-	0.24	100.91	0	2	97
AL8	rhy	alk feld	gm	64.46	18.51	-	-	0.08	15.66	0.25	0.35	99.32	0	2	98
AL8	rhy	alk feld	gm	64.48	18.13	0.18	0.21	0.13	15.72	0.75	0.34	99.94	1	2	97

pl = plagioclase; alk feld = alkali feldspar; mcr = microphenocryst; gm = groundmass. An, Ab and Or in mol%.
gph = granophyre; b.a. = basaltic andesite; xen = xenolith in BR4 sample; rhy = rhyolite. Samples BR4 (mafic) and AL4 (rhyolitic) are dykes.

Table 2: Representative chemical analyses (in wt.%) of pyroxenes in the Barda rocks, Saurashtra

Sample	Rock name	Mineral name	Description	SiO_2	TiO_2	Al_2O_3	FeO	MnO	MgO	CaO	Na_2O	Cr_2O_3	V_2O_3	Sum	Mg#	Di-Hd	En-Fs	Ac	Jd
BR3	gph	cpx	mcr	47.24	0.52	0.66	29.59	1.79	-	19.95	0.98	-	0.24	100.96	0	0.86	0.08	0.08	0.00
BR3	gph	cpx	mcr	46.82	-	0.50	29.55	1.42	0.05	20.48	0.88	0.03	-	99.73	0	0.90	0.07	0.07	0.00
BR3	gph	cpx	core	46.81	0.40	0.69	30.62	1.26	0.02	19.88	1.03	0.09	-	100.80	0	0.86	0.10	0.08	0.00
BR3	gph	cpx	rim	46.52	0.63	0.50	29.31	1.68	-	20.27	1.03	0.02	-	99.98	0	0.88	0.07	0.08	0.00
BR3	gph	cpx	rim	47.38	0.28	0.42	30.08	1.50	0.14	19.78	0.79	-	0.11	100.46	1	0.86	0.09	0.06	0.00
BR3	gph	cpx	core	46.48	0.44	0.52	29.50	1.72	0.18	20.02	1.02	-	-	99.88	1	0.87	0.09	0.08	0.00
BR3	gph	cpx	rim	46.87	0.29	0.66	29.82	1.45	0.10	19.77	0.85	-	-	99.80	1	0.86	0.09	0.07	0.00
BR7	gph	cpx	mcr	47.35	0.30	0.29	30.65	0.98	0.04	19.11	1.82	0.28	-	100.83	0	0.83	0.12	0.15	0.00
BR7	gph	cpx	mcr	47.13	0.35	0.56	30.41	1.11	-	18.99	1.75	-	0.07	100.37	0	0.83	0.12	0.14	0.00
BR7	gph	cpx	mcr	47.92	0.24	0.37	30.10	1.60	0.14	17.93	2.04	0.05	-	100.41	1	0.79	0.13	0.16	0.00
BR7	gph	cpx	mcr	47.09	0.32	0.31	30.58	1.59	-	18.69	1.94	0.11	-	100.62	0	0.81	0.13	0.16	0.00
BR7	gph	cpx	mcr	47.04	0.26	0.32	30.54	1.56	0.15	18.81	1.72	0.16	0.09	100.64	1	0.82	0.13	0.14	0.00
BR7	gph	cpx	mcr	48.24	0.56	0.34	29.78	1.22	-	18.72	1.83	0.09	0.03	100.81	0	0.82	0.10	0.12	0.00
BR12	gph	cpx	mcr	48.76	0.00	0.45	29.48	2.99	0.02	15.56	3.38	0.06	-	100.69	0	0.69	0.17	0.23	0.03
BR12	gph	cpx	mcr	49.20	0.21	0.36	29.76	1.68	-	14.91	4.61	-	0.11	100.85	0	0.66	0.18	0.30	0.04
BR12	gph	cpx	mcr	49.22	0.14	0.51	30.46	0.88	-	15.01	4.36	-	-	100.58	0	0.66	0.19	0.27	0.05
BR11	gph	cpx	core	47.17	0.59	0.67	30.26	1.33	0.07	20.05	0.07	0.21	-	100.42	0	0.87	0.09	0.01	0.00
BR11	gph	cpx	core	46.84	0.60	0.43	31.63	1.02	0.17	19.61	-	-	0.40	100.69	1	0.85	0.13	0.00	0.00
BR11	gph	cpx	rim	47.02	0.28	0.75	30.50	1.08	0.15	19.49	0.29	-	0.26	99.80	1	0.85	0.11	0.02	0.00
BR11	gph	cpx	core	46.98	0.54	0.71	29.39	0.98	0.19	20.17	0.51	-	-	99.47	1	0.88	0.08	0.04	0.00
BR11	gph	cpx	core	46.89	0.66	0.39	29.79	0.97	0.18	19.99	0.17	-	-	99.03	1	0.88	0.09	0.01	0.00
BR11	gph	cpx	mcr	47.31	0.54	0.43	29.20	2.21	0.07	19.93	0.24	0.15	-	100.07	0	0.87	0.07	0.02	0.00
BR11	gph	cpx	core	47.13	0.83	0.16	30.34	1.43	0.07	18.66	0.57	0.17	-	99.36	0	0.83	0.12	0.02	0.00
BR4	b.a.	opx	gm	53.24	0.14	0.67	20.70	0.88	24.35	0.83	-	0.15	-	100.96	68	0.01	0.98	0.00	0.00
BR4	b.a.	opx	gm	52.72	0.87	0.79	20.23	0.94	23.47	1.13	-	0.23	-	100.38	67	0.02	0.95	0.00	0.00
BR4	b.a.	opx	gm	53.32	0.13	0.69	18.87	0.76	23.97	1.53	-	0.03	-	99.29	69	0.05	0.93	0.00	0.00
BR4	b.a.	opx	gm	53.05	0.13	0.85	19.77	0.58	24.38	0.87	-	0.19	-	99.81	69	0.02	0.97	0.00	0.00
BR4	b.a.	opx	gm	53.27	0.19	0.50	20.57	0.68	24.38	0.80	-	-	0.15	100.55	68	0.01	0.98	0.00	0.00
BR4	b.a.	opx	gm	53.73	0.09	0.64	19.67	0.63	23.87	1.22	-	-	0.23	100.09	68	0.03	0.94	0.00	0.00
BR4	b.a.	cpx	gm	54.36	0.50	0.87	8.60	0.25	14.60	20.33	0.19	-	-	99.71	75	0.77	0.15	0.00	0.01
BR4	b.a.	cpx	gm	52.77	0.27	0.95	8.78	0.51	14.87	20.92	0.09	-	0.23	99.39	75	0.82	0.14	0.00	0.01
BR4	b.a.	cpx	gm	52.78	0.31	1.03	9.11	0.55	15.64	20.34	0.03	0.10	-	99.89	75	0.79	0.18	0.00	0.00
BR4	b.a.	cpx	mcr	52.70	0.35	1.12	9.49	0.54	14.40	21.05	-	-	-	99.64	73	0.82	0.14	0.00	0.00
BR4	b.a.	cpx	gm	53.03	0.47	0.89	8.70	0.34	15.01	21.29	0.06	0.08	-	99.85	75	0.83	0.14	0.00	0.00
BR4	xen	opx	core	53.31	-	0.73	19.54	0.55	24.26	1.44	-	-	0.12	99.95	69	0.04	0.95	0.00	0.00
BR4	xen	opx	core	52.87	0.17	1.07	19.49	0.42	24.14	1.24	-	-	0.18	99.57	69	0.03	0.96	0.00	0.00
BR4	xen	opx	core	53.51	0.33	0.79	19.20	0.62	24.36	1.07	-	-	0.08	99.96	69	0.02	0.95	0.00	0.00

gph = granophyre; b.a. = basaltic andesite; xen = xenolith in BR4 sample. mcr = microphenocryst; gm = groundmass; opx = orthopyroxene; cpx = clinopyroxene. Mg# = atomic 100*(Mg+Fe)
Pyroxene components: Di-Hd = Diopside-Hedenbergite; En-Fs = Enstatite-Ferrosilite; Ac = Acmite; Jd =Jadeite.

Table 3: Representative chemical analyses (in wt.%) of magnetites and ilmenites in the Barda rocks, Saurashtra

Sample	Rock name	Mineral name	Description	TiO_2	Al_2O_3	Fe_2O_3	FeO	MnO	MgO	Cr_2O_3	V_2O_3	NiO	Sum	Ulv	Ilm
BR3	gph	mgt	core	6.85	0.64	54.65	36.83	0.57	-	-	0.11	0.11	99.75	20	-
BR3	gph	mgt	core	16.85	0.43	35.58	44.93	1.79	-	0.10	0.14	-	99.82	48	-
BR3	gph	mgt	core	12.03	0.29	45.66	41.45	0.90	0.02	-	0.03	0.09	100.47	34	-
BR3	gph	mgt	core	1.65	0.41	64.93	32.31	0.18	-	-	0.06	-	99.53	5	-
BR5	gph	mgt	core	0.95	0.05	67.65	31.99	0.20	-	-	-	-	100.84	3	-
BR5	gph	mgt	core	1.27	0.30	65.86	31.47	0.68	-	-	0.05	0.52	100.16	4	-
BR5	gph	mgt	core	1.25	0.11	66.68	31.77	0.33	0.15	-	0.09	-	100.38	4	-
BR5	gph	mgt	core	0.95	0.04	66.59	31.15	0.27	0.21	-	0.18	-	99.39	3	-
BR7	gph	mgt	core	10.06	0.20	49.04	38.21	2.12	-	-	0.10	0.26	99.98	28	-
BR7	gph	mgt	core	13.29	0.42	42.92	42.34	1.21	-	0.04	0.06	0.27	100.57	38	-
BR12	gph	mgt	core	24.37	0.19	21.92	52.84	1.15	-	-	0.36	-	100.81	69	-
BR4	b.a.	mgt	core	4.44	1.15	57.75	34.33	0.09	0.61	0.99	0.54	0.11	100.01	13	-
BR4	b.a.	mgt	core	3.67	1.25	58.80	33.61	0.29	0.49	1.53	0.23	-	99.87	11	-
BR5	gph	ilm	mcr	49.68	-	4.59	36.56	8.03	-	-	0.76	-	99.62	-	95
BR5	gph	ilm	mcr	48.26	0.10	8.51	33.37	9.91	-	-	0.65	-	100.80	-	91
BR5	gph	ilm	mcr	47.58	-	8.80	34.81	7.89	-	0.47	0.04	-	99.59	-	91
BR7	gph	ilm	incl	49.55	0.25	6.37	41.56	2.93	0.02	0.10	0.07	-	100.85	-	94
BR4	b.a.	ilm	gm	46.38	0.28	12.55	37.40	0.72	2.02	-	0.43	-	99.78	-	87
BR4	b.a.	ilm	gm	44.82	0.10	14.83	34.97	0.98	2.45	-	0.88	0.62	99.65	-	85
BR4	b.a.	ilm	gm	46.46	0.15	11.83	37.84	1.73	1.23	-	0.40	-	99.64	-	88
BR4	b.a.	ilm	gm	46.44	0.04	12.40	37.91	1.36	1.40	-	0.18	0.23	99.96	-	88

gph = granophyre; b.a. = basaltic andesite; gm = groundmass; incl = inclusion; mcr = microphenocryst; mgt = magnetite; ilm = ilmenite. Ulv = ulvöspinel mol.%; Ilm = ilmenite mol.%

Table 4: Representative chemical analyses (in wt.%) of zircons, titanites, apatites and monazites in the Barda-Alech rocks, Saurashtra

Sample	Rock name	mineral name	Description	SiO_2	TiO_2	Al_2O_3	FeO	MnO	CaO	Na_2O	P_2O_5	SrO	Zr	Nb	La	Ce	Nd	Sm	Hf	Th	F	Cl	S	Sum
BR3	gph	zircon	incl	32.33	-	-	-	-	-	-	-	-	66.74	-	-	-	-	-	0.12	-	-	-	-	99.20
BR3	gph	zircon	incl	31.83	-	-	0.26	-	-	-	-	-	65.86	-	-	-	-	-	1.55	-	-	-	-	99.50
BR7	gph	zircon	mcr	31.43	-	-	0.13	-	-	-	-	-	65.42	-	-	-	-	-	1.92	-	-	-	-	98.90
BR7	gph	zircon	mcr	32.08	-	-	-	-	-	-	-	-	65.79	-	-	-	-	-	2.38	-	-	-	-	100.25
BR5	gph	titanite	mcr	30.92	29.06	4.07	5.29	-	28.04	0.49	-	0.24	-	0.07	0.27	0.13	-	-	-	-	-	-	-	98.58
BR5	gph	titanite	mcr	29.71	30.24	0.84	4.98	-	25.63	0.67	-	-	0.27	2.28	0.89	0.42	1.25	0.56	-	0.28	-	-	-	98.04
BR5	gph	titanite	mcr	31.66	28.58	5.26	5.65	-	27.47	0.53	-	-			0.16	0.07			-	-	-	-	-	99.38
BR5	gph	titanite	mcr	31.40	27.18	5.55	4.14	0.17	28.17	0.41	-	-	-	-	1.59	-	0.53	0.38	-	0.11	-	-	-	99.64
BR5	gph	titanite	mcr	29.79	38.25	0.16	1.61	0.40	28.23	0.54	-	0.04	0.27	0.70	0.42	0.16	0.13	0.35	-	0.06	-	-	-	101.11
BR7	gph	titanite	mcr	28.89	28.75	0.60	6.05	0.06	26.14	0.80	-	-	-	3.74	1.91	1.37	0.72	-	-	0.16	-	-	-	99.16
AL2	rhy	apatite	incl	0.28	-	-	0.90	-	55.19	-	41.63	1.30	-	-	-	-	-	-	-	-	1.08	0.07	0.58	99.31
AL2	rhy	apatite	incl	0.83	-	-	0.77	-	55.06	-	41.18	1.14	-	-	-	-	-	-	-	-	-	-	0.26	98.99
AL9	rhy	monazite	gm	2.08	-	-	-	-	0.61	-	27.79	0.67	-	-	20.28	33.99	4.47	-	-	7.39	-	-	0.13	97.27
AL9	rhy	monazite	gm	1.52	-	-	0.60	-	0.21	-	27.88	0.46	-	-	15.05	42.61	9.47	-	-	1.16	-	0.02	0.04	98.95

gph = granophyre; rhy = rhyolite; mcr = microphenocryst; gm = groundmass.

Table 5. Summary of ^{40}Ar-^{39}Ar dating results for granophyres of the Barda complex, Saurashtra

Sample	Plateau					Isochron				Inverse isochron			
	Steps	$\%^{39}Ar$	Age (Ma)	MSWD	*p*	Age (Ma)	Trap	MSWD	*p*	Age (Ma)	Trap	MSWD	*p*
BR3	11	89.4	68.5 ± 0.4	0.85	0.58	68.5 ± 0.6	295.9 ± 2.2	0.31	0.97	68.5 ± 0.5	296.0 ± 1.6	0.78	0.64
BR5	12	81.3	69.9 ± 0.3	0.41	0.95	69.8 ± 0.6	296.6 ± 3.9	0.12	1.00	69.8 ± 0.5	297.0 ± 2.7	0.21	1.00
BR7	7	67.1	69.0 ± 0.5	0.18	0.98	69.0 ± 0.9	295.4 ± 3.8	0.13	0.98	68.9 ± 0.7	295.7 ± 2.8	0.23	0.95

Notes: Trap is initial $^{40}Ar/^{36}Ar$ ratio (trapped component) and MSWD is Mean Square Weighted Deviate and *p* is the corresponding probability. Errors are reported at the 2σ confidence level and monitor mineral is MMHb (523.1 ± 2.6 Ma, Renne *et al*. 1998).

Table 6: Major and trace element data for rocks of the Barda and Alech complexes, Saurashtra

Sample	BR1	BR3	BR4	BR5	BR7	BR11	BR12	AL1	AL3	AL4	AL5	AL7	AL8	AL9	AL10	AL11	W-2a Meas	W-2a Cert	SY-4 Meas	SY-4 Cert	JR-1 Meas	JR-1 Cert
rock type	gph	gph	b.a.	gph	gph	gph	gph	rhy	rhy	rhy	rhy	dac	rhy	rhy	rhy	dac						
SiO_2	70.21	72.92	52.97	72.44	73.04	72.46	71.27	69.82	86.71	71.29	77.28	66.53	69.35	72.56	77.72	65.60	52.48	52.40	49.71	49.90	-	-
TiO_2	0.47	0.35	1.12	0.31	0.29	0.30	0.35	0.35	0.24	0.34	1.02	0.78	0.57	0.23	0.73	1.12	1.06	1.06	0.29	0.29	-	-
Al_2O_3	12.73	11.94	16.99	11.82	11.56	11.82	11.85	13.97	7.03	13.30	12.88	12.24	12.97	11.44	10.43	11.42	15.55	15.40	20.35	20.69	-	-
Fe_2O_{3t}	5.84	4.71	13.52	4.91	4.35	4.45	5.67	3.63	1.03	4.43	1.85	8.87	4.99	5.32	4.40	11.47	10.77	10.70	6.06	6.21	-	-
MnO	0.05	0.09	0.15	0.12	0.07	0.08	0.12	0.03	0.01	0.09	0.05	0.16	0.03	0.04	0.01	0.12	0.17	0.16	0.11	0.11	-	-
MgO	0.16	0.04	4.06	0.07	0.06	0.05	0.08	0.13	0.03	0.07	0.08	0.21	0.61	0.03	0.11	0.22	6.25	6.37	0.51	0.54	-	-
CaO	0.59	1.17	7.23	0.31	1.05	0.92	1.48	0.21	0.22	0.36	0.28	1.96	1.06	0.63	0.13	0.38	11.03	10.90	8.14	8.05	-	-
Na_2O	4.11	4.02	2.56	4.03	3.96	4.03	4.18	3.91	0.03	4.39	0.06	2.94	3.11	3.66	0.03	0.75	2.23	2.14	6.96	7.10	-	-
K_2O	3.83	3.86	0.83	3.80	3.99	3.99	3.55	4.96	0.11	4.77	1.04	3.26	4.31	4.15	0.55	4.29	0.62	0.63	1.66	1.66	-	-
P_2O_5	0.05	0.01	0.04	0.01	0.01	0.01	0.01	0.01	0.02	0.02	0.04	0.20	0.09	0.01	0.15	0.21	0.13	0.13	0.13	0.13	-	-
LOI	1.64	0.41	0.30	1.09	0.86	0.41	1.27	2.06	3.44	1.01	5.51	3.26	2.85	1.47	4.94	4.83	-	-	-	-	-	-
Total	99.69	99.52	99.76	98.90	99.24	98.52	99.82	99.08	98.87	100.07	100.08	100.41	99.94	99.54	99.20	100.42	100.29	99.89	93.91	94.68	-	-
Be	2	3	1	3	3	3	3	3	2	4	2	2	2	14	1	< 1	< 1	1.3	3	2.6	-	-
V	6	< 5	253	7	< 5	< 5	5	5	13	5	10	9	34	8	22	51	266	262	9	8	-	-
Cr	710	630	420	920	930	860	810	430	540	800	100	320	390	490	500	100	90	92	-	-	-	-
Co	2	1	40	2	2	2	2	1	1	2	3	8	4	1	8	22	43	43	-	-	-	-
Ni	20	30	100	< 20	30	50	20	< 20	30	30	< 20	< 20	< 20	< 20	20	< 20	80	70	-	-	< 20	1.67
Cu	560	1190	2070	360	810	2550	610	750	1080	1200	120	450	640	520	540	330	110	110	-	-	< 10	2.68
Zn	450	850	1250	300	670	1440	470	610	750	810	90	360	450	520	260	220	80	80	-	-	30	30.6
Ga	21	21	19	20	20	21	20	24	19	23	20	19	18	34	18	18	18	17	-	-	15	16.1
Ge	1	2	2	1	2	2	2	1	2	2	1	2	1	2	2	1	2	1	-	-	2	1.88
As	< 5	< 5	< 5	< 5	< 5	< 5	< 5	< 5	< 5	< 5	< 5	< 5	< 5	< 5	< 5	< 5	< 5	1.2	-	-	15	16.3
Rb	122	123	36	117	127	126	104	143	5	145	23	78	101	377	20	87	20	21	-	-	252	257
Sr	84	65	135	62	65	52	69	43	67	59	18	77	72	18	191	157	200	190	1194	1191	-	-
Y	112	108	24	87	103	102	102	109	89	106	73	63	67	291	53	43	20	24	117	119	-	-
Zr	447	557	123	454	523	525	495	610	647	584	357	336	384	2650	300	282	95	94	538	517	-	-
Nb	49	55	5	50	52	53	55	108	123	108	27	26	26	852	20	21	-	-	-	-	15	15.2
Mo	6	6	2	6	7	7	7	4	18	8	< 2	3	3	7	6	2	< 2	0.6	-	-	3	3.25
Sn	17	28	42	11	22	56	16	21	29	29	5	11	15	39	9	6	-	-	-	-	3	2.86
Cs	1.6	2.1	1.3	1.7	2.1	2	1.7	0.9	< 0.5	1.4	< 0.5	1.5	1.5	2.7	< 0.5	0.6	-	-	-	-	20.6	20.8
Ba	921	951	244	1034	895	944	915	1259	132	1782	385	833	1059	85	471	1481	173	182	348	340	-	-
La	83.6	66.5	14.1	50.4	63.5	64.6	61.1	119	93	84.2	48.5	42.7	45.1	254	39.2	35.7	10.1	10	-	-	19	19.7
Ce	126	130	31.9	117	124	128	120	146	170	153	95.1	85.6	88.5	475	77.2	71.5	24.3	23	-	-	44.9	47.2
Pr	16.9	14.3	3.64	11.6	13.5	13.9	13.3	23.6	18.3	16.5	10.9	9.62	10.2	48.4	9.36	7.96	-	-	-	-	5.6	5.58
Nd	64.2	54.2	15.3	44.1	50.1	53.5	51.3	86.6	64	61.7	42.9	37	38.3	160	35.7	30.1	13.2	13	-	-	21.9	23.3
Sm	13.9	12.5	4.1	10.3	11.5	12.1	11.4	17.7	11.4	12.5	9.6	8.2	8.8	32.8	7.6	6.3	3.4	3.3	-	-	5.5	6.03
Eu	3.17	2.31	1.16	2.60	1.94	2.19	2.65	3.62	0.71	2.72	2.30	2.07	1.84	0.44	1.88	1.56	-	-	-	-	0.27	0.3
Gd	15.60	14.10	4.60	11.50	13.00	13.50	13.10	18.00	10.60	13.80	10.20	9.10	9.50	33.90	8.00	6.30	-	-	-	-	5.5	5.06
Tb	2.80	2.70	0.80	2.20	2.40	2.60	2.50	3.00	2.10	2.50	1.80	1.60	1.60	6.60	1.30	1.10	0.6	0.63	-	-	1.1	1.01
Dy	18.50	18.70	5.10	15.80	17.10	17.80	17.00	19.80	14.80	17.00	12.40	11.10	11.20	45.70	8.90	7.60	-	-	-	-	6	5.69
Ho	4.10	4.10	1.10	3.50	3.80	4.00	3.70	4.10	3.40	3.80	2.70	2.40	2.40	10.10	2.00	1.80	0.8	0.76	-	-	-	-
Er	12.40	12.80	3.00	11.20	11.70	12.20	11.60	12.60	10.50	11.90	8.00	7.20	7.30	31.80	6.00	5.50	-	-	-	-	-	-
Tm	1.89	1.99	0.45	1.76	1.84	1.92	1.79	1.97	1.64	1.88	1.22	1.11	1.12	5.02	0.97	0.86	-	-	-	-	0.62	0.67
Yb	12.50	13.40	3.00	12.40	12.70	13.00	12.80	14.10	11.20	13.10	8.60	7.70	7.90	33.80	6.50	5.90	2.1	2.1	-	-	4.6	4.55
Lu	1.93	2.06	0.48	1.95	1.96	2.01	2.02	2.37	1.75	2.17	1.38	1.25	1.26	5.13	1.02	0.95	0.31	0.33	-	-	0.7	0.71
Hf	10.0	12.4	3.0	10.1	11.7	11.7	10.8	13.2	13.7	12.5	8.0	7.7	8.8	59.2	6.1	6.1	-	-	-	-	4.4	4.51
Ta	3.8	4.4	0.4	4.0	4.4	4.2	4.2	8.8	11.6	8.3	1.9	1.8	1.9	72.1	1.5	1.5	0.5	0.5	-	-	2	1.86
W	1	2	< 1	1	1	2	2	2	1	1	3	2	1	5	2	2	< 1	0.3	-	-	2	1.59
Pb	53	84	144	27	65	127	57	45	67	71	17	33	53	66	22	26	-	-	-	-	18	19.3
Bi	< 0.4	< 0.4	< 0.4	< 0.4	< 0.4	< 0.4	< 0.4	< 0.4	< 0.4	0.4	< 0.4	< 0.4	< 0.4	< 0.4	< 0.4	< 0.4	< 0.4	0.03	-	-	0.6	0.56
Th	14.5	16.8	4.3	13.9	16.2	16.3	14.9	18.4	18.1	17.2	10.1	9.5	11.4	124	8.1	7.5	2.4	2.4	-	-	25.4	26.7
U	2.5	3.7	0.3	2.8	3.1	3.6	3.6	3.9	4.5	3.6	2.3	1.9	2.5	27.4	1.8	1.6	0.5	0.53	-	-	8.6	8.88

Notes: Major oxides are in weight percent and trace elements in parts per million (ppm). Rock names (gph, granophyre; b.a., basaltic andesite; rhy, rhyolite and dac, dacite) are from the SINCLAS program of Verma, Torres-Alvarado & Sotelo-Rodriguez (2002) which uses LOI-free recalculated data and the TAS diagram of Le Bas *et al*. (1986). Samples BR4, AL4 and AL11 are dykes. LOI is loss in weight on ignition.
"Cert." are the recommended values and "Meas." the measured values on USGS and CANMET reference materials.

Table 7. Sr and Nd isotopic data for rocks of the Barda and Alech complexes, Saurashtra

Location	Barda	Barda	Barda	Barda	Barda	Barda	Barda	Alech	Alech	Alech	Alech	Alech
Rock type	Granophyre	Granophyre	Basaltic andesite	Granophyre	Granophyre	Granophyre	Granophyre	Rhyolite	Rhyolite	Dacite	Rhyolite	Dacite
Sample	**BR1**	**BR3**	**BR4**	**BR5**	**BR7**	**BR11**	**BR12**	**AL4**	**AL5**	**AL7**	**AL10**	**AL11**
Rb ppm	122	123	36	117	127	126	104	145	23	78	20	87
Sr ppm	84	65	135	62	65	52	69	59	18	77	191	157
Rb/Sr	1.452	1.892	0.267	1.887	1.954	2.423	1.507	2.458	1.278	1.013	0.105	0.554
$^{87}Rb/^{86}Sr$	4.203	5.476	0.772	5.461	5.654	7.011	4.361	7.111	3.697	2.931	0.303	1.603
$(^{87}Sr/^{86}Sr)_p$	0.709946	0.711044	0.708104	0.711102	na	na	0.710204	0.712463	0.710794	0.709163	0.706740	0.707842
±	0.000020	0.000020	0.000020	0.000020			0.000020	0.000020	0.000020	0.000020	0.000020	0.000020
$(^{87}Sr/^{86}Sr)_t$	0.706066	0.705988	0.707391	0.706060	na	na	0.706177	0.705897	0.707380	0.706457	0.706460	0.706361
Nd ppm	13.90	12.50	4.10	10.30	11.50	12.10	11.40	12.50	9.60	8.20	7.60	6.30
Sm ppm	64.20	54.20	15.30	44.10	50.10	53.50	51.30	61.70	42.90	37.00	35.70	30.10
Sm/Nd	0.2165	0.2306	0.2680	0.2336	0.2295	0.2262	0.2222	0.2026	0.2238	0.2216	0.2129	0.2093
$^{147}Sm/^{144}Nd$	0.1309	0.1394	0.1620	0.1412	0.1388	0.1367	0.1344	0.1225	0.1353	0.1340	0.1287	0.1265
$(^{143}Nd/^{144}Nd)_p$	0.512611	0.512673	0.511065	0.512661	0.512640	0.512667	0.512626	0.512707	0.512542	0.512562	0.512571	0.512571
±	0.000060	0.000060	0.000060	0.000060	0.000060	0.000060	0.000060	0.000060	0.000060	0.000060	0.000060	0.000060
$(^{143}Nd/^{144}Nd)_t$	0.512556	0.512614	0.510996	0.512601	0.512581	0.512609	0.512569	0.512655	0.512485	0.512505	0.512516	0.512517
εNd_p	–0.5	0.7	–30.7	0.4	0.0	0.6	–0.2	1.3	–1.9	–1.5	–1.3	–1.3
εNd_t	0.0	1.2	–30.4	0.9	0.5	1.1	0.3	2.0	–1.4	–1.0	–0.7	–0.7

Notes: Samples BR4 (basaltic andesite), AL4 (rhyolite), and AL11 (dacite) are dykes. The Sr and Nd isotopic data are age-corrected to 65 Ma using ICPMS values of Rb, Sr, Sm and Nd. Epsilon Nd (ε_{Nd}) values have been calculated for the rocks using a chondritic average value of $^{143}Nd/^{144}Nd = 0.512638$ and $^{147}Sm/^{144}Nd = 0.1967$ (present-day), which gives initial (at 65 million years) chondritic average value of $^{143}Nd/^{144}Nd = 0.512553$. Using the ages obtained in this study (such as 68.5 Ma for sample BR3, instead of 65 Ma) makes no difference to the $\varepsilon_{Nd}t$ values, in particular. Since most samples are not dated, 65 Ma is the preferred age for correcting present-day ratios and for direct comparison with previous studies. "na" indicates not analyzed/available.

Cucciniello, Choudhary, Pande & Sheth

Mineralogy, geochemistry and ^{40}Ar-^{39}Ar geochronology of the Barda and Alech complexes, Saurashtra, northwestern Deccan Traps: Early silicic magmas derived by flood basalt fractionation

Supplementary Table S1
Stepwise $^{40}Ar/^{39}Ar$ data

BR3 WR (Barda granophyre, whole-rock)

Argon isotopic composition (corrected for blank, mass discrimination and interference), Apparent Age and percentage of nucleogenic and radiogenic argon for sample BR3 WR. Errors on age are without and (with) error on J respectively. Errors quoted are 2σ. **J=0.000480± 0.000002**

Temp.° C	$^{36}Ar/^{39}Ar$ (±2σ)	$^{40}Ar/^{39}Ar$ (±2σ)	App.Age(Ma) (±2σ)	^{39}Ar %	$^{40}Ar^{*}$ %	$^{37}Ar/^{39}Ar$ (±2σ)	$^{40}Ar/^{36}Ar$ (±2σ)
400	1.93708	573.168	0.7	0.35	0.14	0.2160	295.9
	0.13729	40.013	49.3 (49.3)			0.0082	41.7
450	9.14641	2709.410	5.8	0.51	0.25	0.2167	296.2
	0.08015	23.314	28.7 (28.7)			0.0090	5.1
500	13.16310	3889.910	0.2	0.58	0.01	0.3165	295.5
	0.23293	69.397	84.6 (84.6)			0.0059	10.1
550	2.64834	802.137	16.9	1.93	2.44	0.2207	302.9
	0.17786	53.044	64.0 (64.0)			0.0047	34.4
600	1.39935	427.555	12.13	2.54	3.29	0.1885	305.6
	0.01420	4.217	5.11 (5.11)			0.0021	5.7
650	1.26914	424.437	42.26	3.15	11.64	0.1139	334.4
	0.00492	2.122	2.17 (2.19)			0.0010	2.5
700	1.22290	442.326	68.72	6.15	18.3	0.0407	361.7
	0.00609	2.266	2.41 (2.43)			0.0007	4.3
750	0.59544	257.157	68.92	10.32	31.58	0.0327	431.9
	0.00132	1.286	1.12 (1.17)			0.0002	2.7
800	0.05991	98.855	68.88	6.83	82.1	0.0445	1650.5
	0.00021	0.494	0.41 (0.54)			0.0008	11.5
850	0.07213	101.507	68.09	10.34	79.01	0.0642	1407.8
	0.00039	0.542	0.46 (0.57)			0.0007	14.6
900	0.13170	119.323	68.26	8.52	67.39	0.0701	906.2
	0.00033	0.597	0.50 (0.61)			0.0011	5.7
950	0.22465	146.967	68.41	7.66	54.83	0.0630	654.2
	0.00129	0.881	0.80 (0.87)			0.0006	7.6
1000	0.28913	166.325	68.67	7.71	48.64	0.0870	575.3
	0.00128	0.832	0.76 (0.83)			0.0006	5.7
1050	0.34291	181.996	68.53	14.15	44.34	0.3011	530.9

	0.00131	0.910	0.82 (0.89)			0.0006	4.2
1100	0.41128	202.458	68.7	12.41	39.98	0.0885	492.3
	0.00094	1.012	0.87 (0.94)			0.0006	3.0
1150	0.40533	200.507	68.56	3.94	40.27	0.1745	494.8
	0.00587	2.771	2.72 (2.75)			0.0007	13.3
1200	0.67349	279.634	68.48	1.38	28.84	0.2690	415.3
	0.01285	5.252	5.40 (5.41)			0.0049	20.2
1250	1.32777	407.965	13.5	0.39	3.83	0.2289	307.3
	0.07268	22.264	26.6 (26.6)			0.0091	31.7
1300	1.76901	553.696	26.6	0.49	5.59	0.2047	313.0
	0.03491	11.090	12.9 (12.9)			0.0064	12.9
1350	2.26417	711.099	36.1	0.64	5.92	0.3929	314.1
	0.15399	48.760	56.6 (56.6)			0.0160	56.2
TOTAL	0.60871	254.895	63.78	100.00	29.44	0.1180	418.8
	0.00394	1.212	1.40 (1.44)			0.0003	3.5

BR5 WR (Barda granophyre, whole-rock)

Argon isotopic composition (corrected for blank, mass discrimination and interference), Apparent Age and percentage of nucleogenic and radiogenic argon for sample BR5 WR. Errors on age are without and (with) error on J respectively. Errors quoted are 2σ. **J=0.000490±0.000003**

Temp.° C	**$^{36}Ar/^{39}Ar$ (±2σ)**	**$^{40}Ar/^{39}Ar$ (±2σ)**	**App.Age(Ma) (±2σ)**	**^{39}Ar %**	**$^{40}Ar^{*}$ %**	**$^{37}Ar/^{39}Ar$ (±2σ)**	**$^{40}Ar/^{36}Ar$ (±2σ)**
450	1.72770	512.202	1.5	0.85	0.33	0.3184	296.5
	0.17318	50.994	63.8 (63.8)			0.0095	47.5
500	4.87395	1445.390	4.6	1.14	0.36	0.3266	296.6
	0.25700	75.698	94.5 (94.5)			0.0091	27.8
550	1.46190	433.514	1.4	3.02	0.36	0.2954	296.6
	0.07088	20.998	26.2 (26.2)			0.0045	24.0
600	1.41760	444.662	22.65	1.86	5.80	0.2420	313.7
	0.02489	8.379	9.73 (9.73)			0.0044	12.6
650	0.32891	143.720	40.66	3.93	32.38	0.1189	437.0
	0.00743	3.380	3.48 (3.49)			0.0029	21.1
700	0.10480	97.944	58.23	7.93	68.39	0.0554	934.8
	0.00070	0.767	0.68 (0.74)			0.0019	14.1
750	0.04050	92.281	69.6	9.53	87.04	0.0695	2280.5
	0.00049	1.176	1.01 (1.06)			0.0022	60.8
800	0.03122	89.601	69.65	10.40	89.71	0.0340	2871.5

	0.00017	0.448	0.38 (0.52)			0.0009	28.0
850	0.05693	97.326	69.76	6.64	82.72	0.0309	1710.0
	0.00015	0.487	0.42 (0.54)			0.0002	11.3
900	0.10229	111.010	70	5.36	72.78	0.0400	1085.4
	0.00024	0.555	0.48 (0.59)			0.0006	7.0
950	0.14671	124.070	69.94	5.34	65.06	0.0298	845.7
	0.00037	0.620	0.54 (0.64)			0.0006	5.3
1000	0.14362	123.147	69.93	5.93	65.54	0.0211	857.5
	0.00058	0.616	0.54 (0.65)			0.0005	6.9
1050	0.10523	111.967	70.07	9.46	72.23	0.0215	1064.1
	0.00034	0.560	0.48 (0.6)			0.0004	7.8
1100	0.12606	118.035	69.99	11.75	68.44	0.0262	936.3
	0.00031	0.590	0.51 (0.62)			0.0003	5.8
1150	0.14277	123.149	70.14	12.54	65.74	0.0255	862.6
	0.00046	0.616	0.54 (0.64)			0.0004	6.2
1200	0.30066	169.755	70.11	2.44	47.67	0.0793	564.7
	0.00078	0.849	0.75 (0.83)			0.0008	3.6
1250	0.59624	256.859	69.92	0.86	31.41	0.1395	430.8
	0.00440	1.866	1.93 (1.96)			0.0042	6.6
1350	0.96245	365.129	69.96	1.03	22.11	0.1111	379.4
	0.02258	8.398	9.12 (9.12)			0.0021	18.7
TOTAL	0.25983	150.089	63.64	100.00	48.85	0.0587	577.7
	0.00397	1.194	1.43 (1.46)			0.0004	10.1

BR7 WR (Barda granophyre, whole-rock)

Argon isotopic composition (corrected for blank, mass discrimination and interference), Apparent Age and percentage of nucleogenic and radiogenic argon for sample BR7 WR. Errors on age are without and (with) error on J respectively. Errors quoted are 2σ. **J=0.000490± 0.000003**

Temp.° C	**$^{36}Ar/^{39}Ar$ (±2σ)**	**$^{40}Ar/^{39}Ar$ (±2σ)**	**App.Age(Ma) (±2σ)**	**^{39}Ar %**	**$^{40}Ar^{*}$ %**	**$^{37}Ar/^{39}Ar$ (±2σ)**	**$^{40}Ar/^{36}Ar$ (±2σ)**
450	1.98570	589.910	2.78	0.66	0.54	0.2779	297.1
	0.02663	7.761	9.71 (9.71)			0.0068	6.9
550	3.32901	984.087	0.4	3.90	0.04	0.2955	295.6
	0.09986	4.920	26.3 (26.3)			0.0054	11.7
600	1.30437	391.399	5.26	4.68	1.53	0.2654	300.1
	0.02303	1.957	6.21 (6.21)			0.0023	7.2
650	1.92083	647.593	69.01	4.15	12.35	0.0555	337.1

	0.02814	3.238	7.55 (7.56)			0.0017	11.6
700	0.80926	319.500	69.32	14.80	25.15	0.0353	394.8
	0.00463	1.598	1.78 (1.81)			0.0010	4.3
750	0.40544	199.619	68.85	17.88	39.98	0.0163	492.4
	0.00100	0.998	0.88 (0.95)			0.0004	4.1
800	0.09728	108.835	69.09	10.12	73.59	0.0337	1118.9
	0.00034	0.544	0.47 (0.58)			0.0005	11.4
850	0.15576	125.882	68.92	6.74	63.45	0.1775	808.6
	0.00038	0.629	0.54 (0.64)			0.0006	5.0
900	0.24398	151.804	68.78	6.22	52.52	0.1232	622.3
	0.00056	0.759	0.66 (0.74)			0.0006	3.9
950	0.29127	166.246	69.17	7.20	48.23	0.0583	570.8
	0.00105	0.831	0.75 (0.83)			0.0006	3.9
1000	0.53469	314.206	132.4	4.08	49.72	0.0921	587.7
	0.00727	4.514	4.09 (4.14)			0.0014	16.4
1050	0.48313	294.277	128.67	7.41	51.51	0.5059	609.4
	0.00406	2.635	2.37 (2.46)			0.0045	10.9
1100	0.69858	362.783	132.54	6.57	43.10	0.1759	519.4
	0.01472	8.033	7.46 (7.49)			0.0028	21.9
1150	0.89864	420.724	131.58	3.30	36.89	0.1780	468.2
	0.00493	2.336	2.25 (2.34)			0.0021	4.3
1200	1.36373	496.993	80.9	0.41	18.92	0.3224	364.5
	0.06622	2.487	16.6 (16.6)			0.0074	35.8
1250	1.44082	538.686	96.73	0.63	20.97	0.3238	373.9
	0.01447	2.694	4.21 (4.24)			0.0098	7.6
1300	1.52856	564.935	96.99	1.25	20.05	0.2908	369.6
	0.02841	2.825	7.38 (7.4)			0.0035	12.9
TOTAL	0.69954	296.238	77.07	100.00	30.22	0.1292	423.5
	0.00442	0.723	1.26 (1.32)			0.0005	3.2

Supplementary Table S2: CIPW norms of the Barda and Alech rocks

Sample	BR1	BR3	BR4	BR5	BR7	BR11	BR12	AL1	AL3	AL4	AL5	AL7	AL8	AL9	AL10	AL11
rock type	gph	gph	b.a.	gph	gph	gph	gph	rhy	rhy	rhy	rhy	dac	rhy	rhy	rhy	dac
qz	27.21	30.24	7.03	31.00	30.74	29.77	27.89	25.61	85.23	24.29	72.00	28.31	29.35	31.19	73.41	38.35
cor	0.87	0.00	0.00	0.54	0.00	0.00	0.00	1.81	6.51	0.31	11.24	0.79	1.48	0.00	9.91	5.35
or	22.63	22.81	4.90	22.45	23.58	23.58	20.98	29.31	0.65	28.19	6.15	19.26	25.47	24.52	3.25	25.35
ab	34.78	34.01	21.66	34.10	33.51	34.10	35.37	33.08	0.25	37.14	0.51	24.88	26.31	30.97	0.25	6.35
an	2.60	3.13	32.42	1.47	1.98	2.38	3.09	0.98	0.96	1.66	1.13	8.42	4.67	2.53	-0.33	0.51
ne	0.00	0.00	0.00	0.00	0.00	0.00	0.00	0.00	0.00	0.00	0.00	0.00	0.00	0.00	0.00	0.00
lc	0.00	0.00	0.00	0.00	0.00	0.00	0.00	0.00	0.00	0.00	0.00	0.00	0.00	0.00	0.00	0.00
ac	0.00	0.00	0.00	0.00	0.00	0.00	0.00	0.00	0.00	0.00	0.00	0.00	0.00	0.00	0.00	0.00
di	0.00	2.32	2.68	0.00	2.81	1.88	3.72	0.00	0.00	0.00	0.00	0.00	0.00	0.48	0.00	0.00
hy	7.16	4.47	24.43	6.14	3.86	4.45	5.10	4.43	1.01	5.43	0.96	10.84	6.98	6.29	4.70	13.54
ol	0.00	0.00	0.00	0.00	0.00	0.00	0.00	0.00	0.00	0.00	0.00	0.00	0.00	0.00	0.00	0.00
mt	1.29	1.04	2.99	1.09	0.96	0.98	1.25	0.80	0.23	0.98	0.41	1.96	1.10	1.18	0.97	2.54
il	0.90	0.66	2.12	0.58	0.55	0.57	0.66	0.66	0.45	0.64	1.93	1.48	1.09	0.44	1.39	2.13
hm	0.00	0.00	0.00	0.00	0.00	0.00	0.00	0.00	0.00	0.00	0.00	0.00	0.00	0.00	0.00	0.00
ap	0.12	0.02	0.09	0.02	0.02	0.02	0.02	0.02	0.05	0.05	0.09	0.47	0.21	0.02	0.36	0.50
aq	1.64	0.41	0.30	1.09	0.86	0.41	1.27	2.06	3.44	1.01	5.51	3.26	2.85	1.47	4.94	4.83
Totale	99.20	99.12	98.62	98.49	98.88	98.14	99.34	98.77	98.78	99.69	99.93	99.67	99.52	99.09	98.84	99.46
A/N+K	1.17	1.11	3.33	1.10	1.07	1.08	1.11	1.18	41.74	1.07	10.52	1.46	1.33	1.09	16.18	1.94
A/CNK	1.06	0.92	0.93	1.04	0.90	0.93	0.88	1.14	12.37	1.01	7.45	1.02	1.10	0.98	11.86	1.74

Rock names (gph, granophyre; b.a., basaltic andesite; rhy, rhyolite and dac, dacite).
The samples AL3, AL5, AL10 and AL11 are altered.
A/CNK = mol Al_2O_3/(CaO+Na_2O+K_2O); A/N+K = mol Al_2O_3/(Na_2O+K_2O).